Chapter 5:

Groundwater Recharge for Tutuila, American Samoa Under Current and Projected Climate as Estimated with SWB2, a Soil Water Balance Model

Abstract

Groundwater is the primary water source on the island Tutuila in American Samoa, and accurate quantification of groundwater availability is essential for well-informed management of this limited resource. A water budget approach using SWB2, a soil water-balance model was applied to Tutuila with the primary objective of calculating spatially and temporally distributed net-infiltration, which directly controls groundwater recharge rate. Other water budget components such as evapotranspiration, canopy interception, runoff, and mountain front recharge were also quantified with the SWB2 model for average present-day climate conditions. Additionally, the potential effects of future climate change on water resources availability were simulated by integrating dynamically downscaled climate predictions for 2080 to 2099 derived from externally supplied global climate model results. Notable improvements in this model over previously developed water budget models for Tutuila include flow-routing based on land topography, inclusion of the mountain front recharge process, and consideration of direct net infiltration from anthropogenic sources such as on-site wastewater units and leaking water delivery lines. Model results indicated approximately 54% of Tutuila's rainfall infiltrates as groundwater recharge, 8% is lost to canopy evaporation, another 15% is lost to evapotranspiration from soils, and 21% is removed through surface-water features as stormflow-runoff. The model was able to simulate these processes with a high-spatial and temporal resolution with a 20 by 20 m grid-cell size, and a daily-resolution output time step. Climate scenarios suggested an increase in net-infiltration of 17 to 27% might be expected by the end of the century depending on the emissions scenario used.

5.1 Introduction

The island of Tutuila in the Territory of American Samoa relies on a limited groundwater supply for almost all of its water needs. In island settings, precipitation rates fundamentally constrain the availability of water. However, for all practical purposes, it is the partitioning of rainfall into different terrestrial reservoirs, along with aquifer storage capacity, that ultimately determines the amount of water accessible for human use. It is this subject, and specifically the quantification of groundwater recharge, that is the primary focus of this report. Accurate assessment of groundwater availability is often limited by uncertainty in the magnitude of recharge, because many critical processes influencing recharge are difficult if not impossible to directly measure. Commonly used approaches for recharge quantification range from simple analytical-regression equations where only limited input data is available (Shade and Nichols, 1996), to highly parameterized watershed models, such as the Soil and Water Assessment Tool (SWAT), which typically require more input data then is often available on regional scales (Arnold et al., 1994). For many applications, mass-balance based water budget models are frequently used to assess recharge and other water budget components on regional, or in this case, island wide scales. Quantitative water-budget models are valuable tools for accomplishing numerous water resource-management goals. including:

- Assessment of surface water availability
- Parameterization of groundwater models, which themselves can be applied in estimating groundwater availability
- Estimation of Submarine Groundwater Discharge (SGD) rates
- Assessing water quality and contaminant transport
- Integrated management of surface and groundwater resources
- Assessing floods and evaluating flooding potential

The water budget method allows integration of long-term climate data with geospatial information to addresses the high-spatial and temporal variability inherent in precipitation and other hydrologic processes found on steep tropical islands. Because groundwater recharge is typically the most difficult water budget component to directly measure, it is often calculated as a residual term after other significant components are subtracted from a metered amount of precipitation. In a simplified form, this approach was formulated by Thornthwaite and Mather (1955) as:

$$Recharge = Rainfall - Runoff - Actual\ Evapotranspiration$$

If it is determined that other inputs or losses, such as irrigation, streamflow infiltration, leaking water delivery lines, or leachate from septic systems are significant, these components can also be included to increase model accuracy. Recent examples of study locales in the Pacific where similar water budget methodologies have been applied include the Hawaiian Islands (Izuka et al., 2016), Guam (Johnson, 2012), and Jeju Island (Mair et al., 2013).

The primary objective for this study is to apply the Soil Water Balance 2 (SWB2) Model (Westenbroek et al., 2018) to create spatially distributed estimates of water balance components on Tutuila with a particular emphasis on groundwater recharge. These estimates are useful for assessing the availability of both groundwater and surface water resources. On Tutuila Island, only three previously documented recharge estimates have been found. These were developed by Eyre and Walker (1991), Izuka et al. (2007), and ASPA (2013). Of the three estimates only one, Izuka et al. (2007), is in a widely available published format, whereas the Eyre and Walker and ASPA water budgets are contained in internal reports, which reside at the ASPA headquarters in Tafuna, American Samoa. These estimates vary in methodology and accuracy of their input datasets, but all generally consider similar water budget components including precipitation, evapotranspiration, runoff, and streamflow infiltration to calculate recharge. However, none of these estimates have attempted to include the effects of leaking water lines or discharge from On-Site wastewater Disposal Systems (OSDS), both of which have the potential to influence localized water budgets significantly.

The first SWB model was originally developed by the U.S. Geological Survey (USGS) Wisconsin Water Science Center in 2010 and is based on a modified Thornthwaite-Mather soil-water balance approach. The SWB2 model is an updated form of the original SWB model with new methods of built in calculation, some of which include functionality from the Hawaii Water Balance Code (Izuka et al., 2010), thereby making it particularly suitable to modeling sites on tropical basaltic islands, such as Tutuila. Water balance components within the model are calculated at a daily-time resolution, and can be averaged into monthly or annual time steps. The model uses a rectangular grid to represent the spatial distribution of variability within the model domain, and the grid resolution can be modified to any desired size based on the resolution of input datasets. Westenbroek et al. (2018) provides detailed information regarding construction and use of the SWB2 model.

While the SWB2 model is applicable in a wide range of climatic and environmental conditions, it features a number of modified methods that are specifically intended to accurately represent hydrologic processes on tropical islands. These include the substitution of monthly runoff coefficients for curve-number generated estimates of runoff, use of Gash canopy interception in place of the bucket method, and modifications to land-use classification parameters that allow modeling of unique environments such as cloud forests. A type example application of the model on the Hawaiian island of Maui was developed for presentation in the SWB2 documentation (Westenbroek et al., 2018), and this example was used as a general guide in the selection of methods for the Tutuila model due to the similar geographic, geologic, and climatic attributes of these tropical island settings.

Datasets specific to the Tutuila model included:

- Gridded monthly precipitation data
- Precipitation gauge data used to represent temporal rainfall distributions
- Land use data
- Impervious surface ratios
- Canopy coverage ratios
- Soil type data consistent with the NRCS SSURGO database
- Geospatial data to represent direct infiltration from municipal water line leaks
- Geospatial data to represent direct infiltration from OSDS effluent discharge
- Watershed runoff-to-rainfall ratios, both measured and interpolated
- Potential evapotranspiration data in monthly gridded format
- Canopy evaporation data
- Gridded monthly maximum and minimum temperature data
- Mountain front recharge information

Details regarding sources and processing of each input dataset are provided in the sections below.

5.1.1 Study Area

The island of Tutuila (Fig. 5.1), located near 14° S and 170° W, is the main population center of American Samoa, and at 142 km^2 is the third largest island in the Samoan hot-spot island chain. Due to its position within the South Pacific Convergence Zone, the island experiences abundant year round rainfall, with increased precipitation amounts from October to May during the wetter season. Monthly average rainfalls in the wet season are roughly twice that of the dry season's still significant rainfall amounts. Rainfall varies considerably with location and elevation and ranges between 70 in./yr. near the Tafuna Airport up to more than 200 in./yr. along the crest of the highest mountains (NWS, 2000). Strong tropical storms and hurricanes also influence the region about once every other year, and an average of 25 to 30 significant thunderstorms affect the island annually (Kennedy et al., 1987). Tutuila consists of two distinct regions: The Tafuna-Leone Plain, a highly-permeable rejuvenated-phase lava delta, which due to its low slope contains concentrated human development; and a mountainous assemblage of Pleistocene age shield volcanoes that make up the bulk of the island and generally consist of lower-permeability rock. (Stearns, 1944).

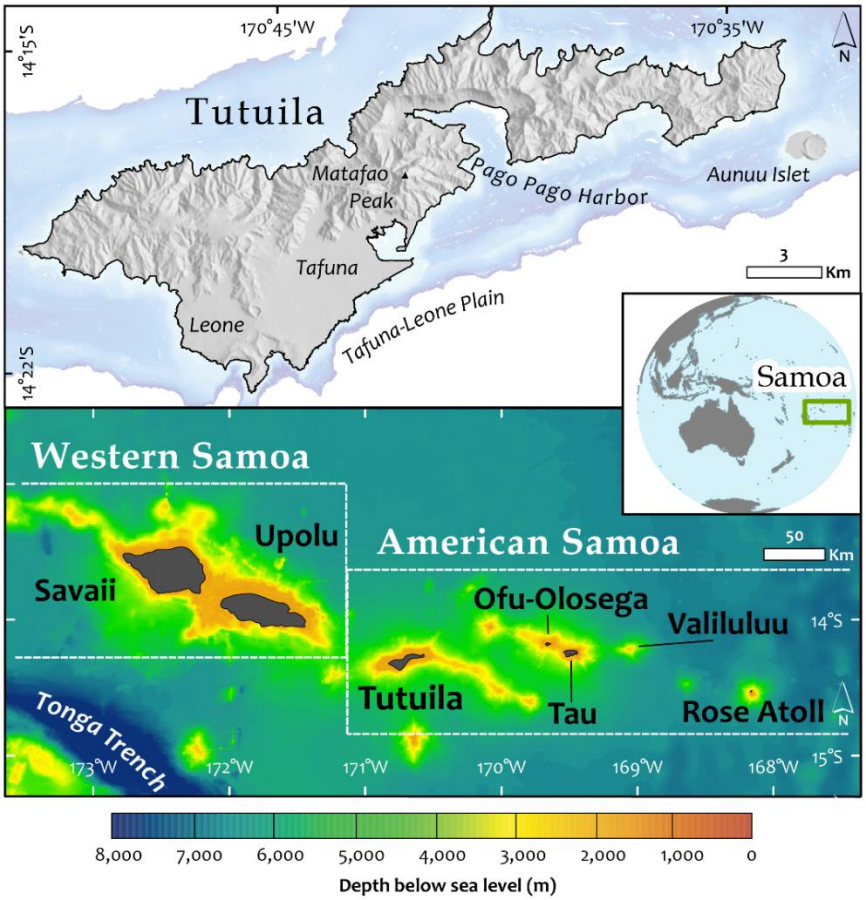

Figure 5.1: Map of Tutuila island (top) and bathymetric map of Samoan archipelago (bottom). Divisions between Western and American Samoa are drawn to mmshow political jurisdictions and do not constitute actual territorial boundaries. Regional location map shown in center-right inset.

5.2 Methods

Compiling and formatting input datasets comprised the bulk of model set up efforts. Except for a portion of the runoff-to-rainfall ratios and rainfall fragment sets, all input datasets used for this model were obtained from existing publications or databases, the details of each having been documented in the respective references cited in this report. Input data for determining rainfall timing and runoff-to-rainfall ratios were compiled from a combination of published and new rainfall and streamflow data collected specifically for use in this work. Where model parameters relating to hydrologic behavior throughout the different land-use and soil zones, specific to American Samoa were not available, the parameters from the Maui Case study were used as, the Hawaiian Islands were considered to be the closest available approximation for Tutuila's soils and land-cover. This approximation was justified because the islands of the Samoan and the Hawaiian island chains are affected by similar climatic patterns as they are both located in the tropics. American Samoa's climate differs from Hawaii in that it is situated closer to the equator and is more affected by the inter-tropical convergence zone.

However, both archipelagos share similar seasonality, steep rainfall gradients, tropical-forested land-cover, and geologic construction.

However, there remains the need for collection of new hydrologic and ecologic data to validate this approximation. The SWB2 model requires all spatially distributed input files to be in the ESRI ascii grid format, and for consistency, all input grids were pre-processed to have consistent boundaries and a 20 m cell-size. The model was run for a period of 10 years in order to average away any potential bias from the default initial soil-moisture conditions.

The SWB2 model runs on a daily time-step, and because of this it is preferred to use gridded daily precipitation data as rainfall input as this yields the most accurate results even when calculating water balance components on monthly or annual scales. However, because these data are not available at sufficient resolution for Tutuila, this application of SWB2 uses a stochastic approach, i.e., the Method of Fragments (described below), to synthesize daily-resolution precipitation data from available monthly precipitation data representing 30-year averages from 1971 to 2000. Rainfall pattern information from rain gauge data spanning the period 1955 to 2018 and streamflow data from 1958 to 2018 used for runoff calculations were also incorporated as model input data. Therefore, this model is rooted in steady-state paradigm, whereas model outputs do not necessarily reflect conditions on any particular day or month, but instead represent average conditions over long-term scales.

It should here be noted that groundwater recharge is defined as water that actually reaches the water table, whereas water-budget and watershed models typically calculate net-infiltration, defined as water that percolates below the root zone. Because vadose zone processes were not modeled as part of this work, it is possible that net-infiltration and groundwater recharge are not strictly equivalent. However, this possibility is typically ignored in basaltic island settings (Engott et al., 2015) because generally high hydraulic conductivities transport water quickly enough to avoid significant evaporative effects within the unsaturated zone. Although the term net-infiltration is often used in this report, it is used interchangeably with groundwater recharge and is intended to refer to the same process.

5.2.1 Gridded Monthly Precipitation

Gridded monthly precipitation data covering the entire island of Tutuila were produced by Oregon State University's PRISM Group using climate records from 1971 to 2000. The processing methodology is documented in Daly et al. (2006), and essentially involved integration of topographic data and rainfall information derived from 21 precipitation observation stations to interpolate a whole-island precipitation grid at a resolution of 90 m cell-size. Gridded precipitation data were produced in ascii grid format and could be directly used in the SWB2 code after pre-processing for cell-size and boundary extent. An example of the gridded data is shown as Fig. 5.2.

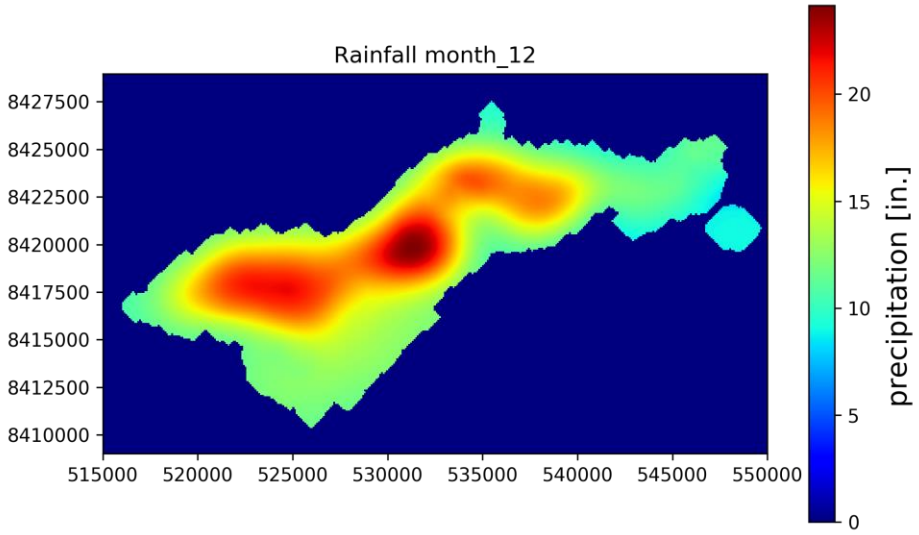

Figure 5.2: Gridded monthly rainfall data for the month of December from Daly et al. (2006). Note map units are in m relative to UTM zone 2S, WGS 84.

5.2.2 Rainfall Fragments

Although the outputs of water budget models are typically presented as monthly or annual totals, SWB2 uses a daily time step for soil moisture calculations, the output of which are subsequently downsampled to obtain monthly or annual results. Therefore, the model requires daily gridded-rainfall data in order to perform the soil-moisture processing step. However, daily gridded rainfall data at sufficient resolution are not currently available for Tutuila. Because this is a common issue on small islands, the SWB2 code contains a built in module to apply the Method of Fragments, which was used in this study to disaggregate the monthly gridded rainfall data (Daly et al., 2006) into daily-gridded rainfall estimates for use in model calculations. The Method of Fragments essentially creates a synthetic daily rainfall series for each modeled month by spreading the total monthly precipitation, taken from the gridded data,

into each day of the month following stochastically selected daily rainfall patterns observed at rain gauges. A synthetic rainfall dataset is created for each rain station, and applied only in the area geographically closest to each station, as defined by Thiessen polygons surrounding the gauge point locations (Fig. 5.3). For a more in-depth explanation of the Method of Fragments and its previous application see Oki (2002) and Westenbroek et al. (2018).

For this study, rainfall patterns or fragment sets were generated with daily precipitation records from 18 distinct rain gauging stations scattered throughout Tutuila. Since the method only indirectly uses rain gauge data, in order to obtain a representative temporal distribution of rain falling throughout the month, rain station periods of record do not need to and did not necessarily overlap. Periods of record for gauges used in this study ranged from 1955 to 2018.

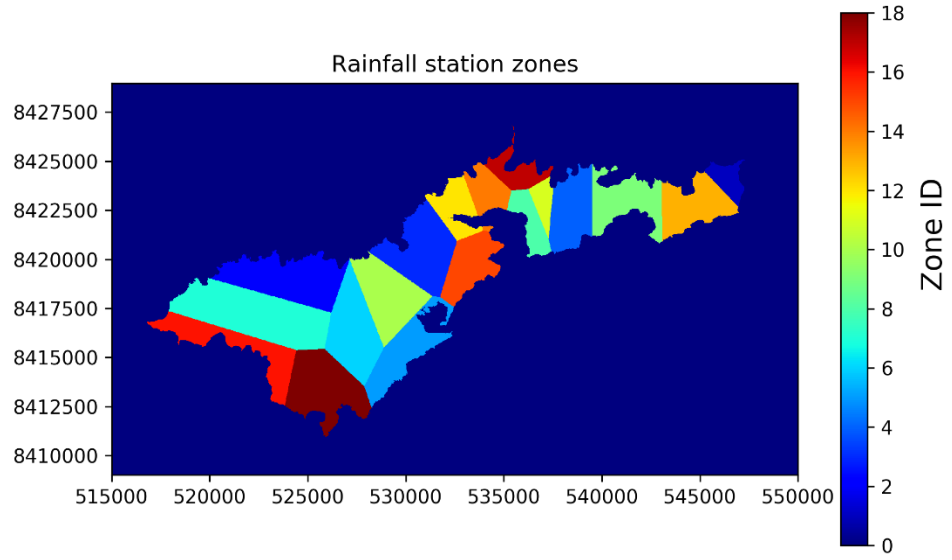

Figure 5.3: Gridded map of 18 rain gauge station zones as defined by the Thiessen polygons, used to define fragment sets for daily rainfall processing.

5.2.3 Land Use

The SWB2 model requires information about the spatial distribution of land use to assign site specific parameters that affect interception or infiltration rates. For this work, land-use data was obtained from a high-resolution wildlife habitat map developed by the American Samoa Department of Marine and Wildlife Resources (DMWR) (Meyer et al., 2016). This map was created using an object-based remote-sensing approach applied to high resolution orthoimagery and LIDAR data collected in 2012, and uses a classification scheme specific to the vegetation of American Samoa. For this study, each distinct land-use type was assigned a zone code, and the vector data supplied by the Meyer work was converted to a raster format, with each land-use type represented as a numerical zone code (Fig. 5.4)

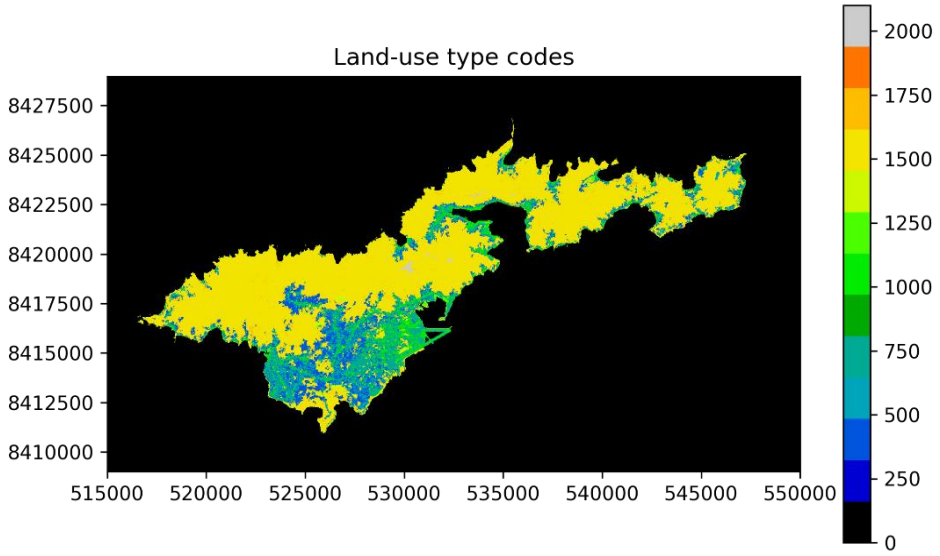

Figure 5.4: Gridded map showing the spatial distribution of different land-use types throughout Tutuila. Land-use code key provided in Table 5.1 below.

The SWB2 model applies parameters for each land-use type by assigning a specific zone code to each land-use and then the model matches these zone codes to parameter sets contained in a separate tabular land-use lookup table. Land-use parameters included rooting zone depth, canopy storage capacity, trunk storage capacity, stem-flow fractions, and certain factors related to irrigation or cropping timing, and those parameters used in the Tutuila model are given in Table 5.1. Because of the geologic and climatic similarities between the Hawaiian Islands and American Samoa, the land-use lookup table from the Maui SWB2 example (Westenbroek et al., 2018) was used to assign parameter values for Tutuila's land uses. Although land-use classifications as defined by Meyer et al. (2016) were not exactly the same as classifications defined in the Maui case, analogous land use types from each model were matched (Table 5.1) to obtain the most-representative parameter values for the Tutuila land-uses.

Table 5.1: Mapping scheme used to transfer land-use parameters from the Maui case as defined in Westenbroek et al. (2018) to land uses in this model as defined by Meyer et al. (2016), and specific parameter values used in the Tutuila SWB2 model.

Tutuila Description ***(Meyer et al., 2016)***	**Land Use Code**	**Maui Description** ***(Westenbroek et al., 2018)***	**Rooting depth [in]**	**Canopy Storage Capacity [in]**	**Trunk Storage Capacity [in]**	**Stemflow Fraction**
Cultivated Land	400	Diversified Agriculture	10	0	0	0
Agroforest	500	Macadamia	60	0	0	0
Open Space	700	Developed Open Space	12	0	0	0
Developed Woodlands	800	Developed Low intensity	12	0	0	0
Buildings, Impervious Surfaces	1000	Developed High intensity	12	0	0	0
Marsh, Mangroves, Swamp	1200	Wetland	39	0	0	0
Landslips, Landfills and Quarries	1300	Sparsely vegetated	5	0	0	0
Grassland/Herbaceous	1400	Grassland	39	0	0	0
Upland Scrub, Coastal Scrub	1500	Shrubland	12	0	0	0
Lowland Rainforest, Coastal Forest	1600	Native forest	30	0.05	0.01	0.04
Successional Scrub Vegetation	1700	Alien forest	60	0.05	0.01	0.04
Montane Rainforest	2100	Native forest fog	30	0.05	0.01	0.04

5.2.4 Soils

The U.S. Natural Resources Conservation Service (NRCS) maintains a standardized database of soil types and properties for soils throughout the U.S. An island-wide soil study of Tutuila was completed by Nakamura (1984) and includes descriptions of each soil type, predictions of soil behavior, and suitability and limitation information of each soil for specified uses. The soil parameters specifically used in the SWB2 model are the hydrologic soil group, which categorizes soils into four groups based on runoff-producing characteristics, and soil moisture capacity, which indicates the total amount of water each soil can hold before losing water to infiltration into aquifer material below. For this study, a georeferenced soil map from Nakamura (1984) was obtained in shapefile format, and was used to develop gridded datasets of hydrologic soil groups (Fig. 5.5) and soil moisture capacity (Fig. 5.6).

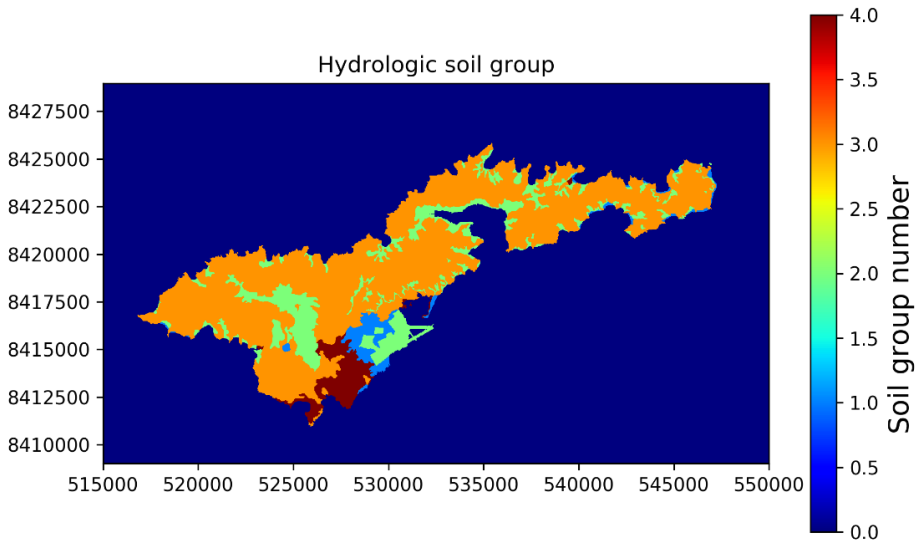

Figure 5.5: Gridded map of hydrologic soil groups derived from Nakamura (1984) for the study area.

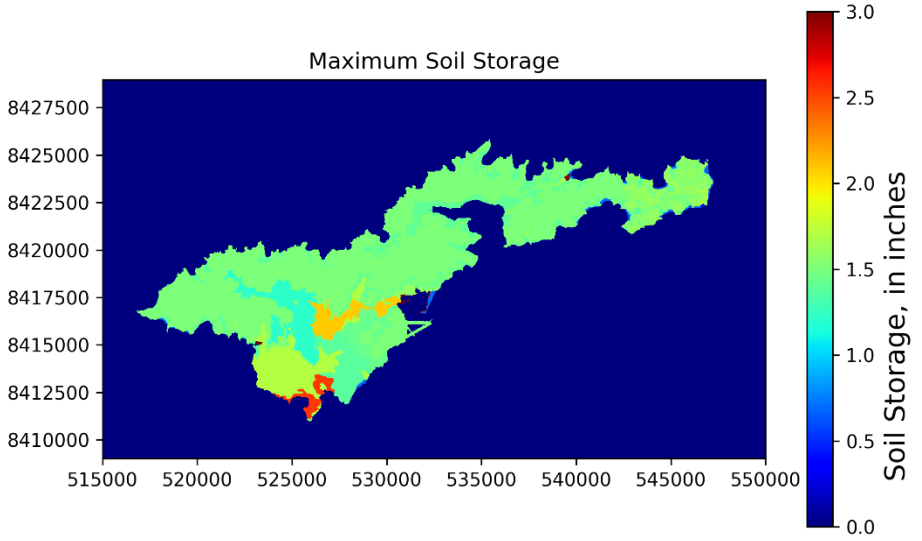

Figure 5.6: Gridded map of soil moisture capacity derived from Nakamura (1984) for the study area.

5.2.5 Runoff to Rainfall Ratios

Starting in the 1960s, the USGS began installation of continuous record stream gauges throughout Tutuila. Between this time and 2008, at least eleven continuous record stream gauges were operated over various periods of record. These data are available at the USGS National Water Information System (NWIS) database (https://waterdata.usgs.gov/aq/nwis/sw) and stream gauging methods are documented in

Wong (1996). However, in 2008, the USGS gauging operations ceased. To fill this data gap and to provide updated data for this study, a collaborative agreement was initiated between University of Hawaii (UH) and ASPA personnel to install eight new stream gauges and begin data collection again. For this study, streamflow data was primarily used in the calculation of runoff-to-rainfall ratios (R:R ratios), which represent the percentage of rainfall that becomes runoff within a given watershed basin, and is removed from the model through an assumed surface water feature. Note that the term runoff as used in this report refers specifically to stormflow generated and lost during and shortly after rainfall events and does not include baseflow, lateral flow, or any other water that has cycled through the aquifer or vadose zone.

To determine R:R ratios in gauged sub-basins, historical USGS streamflow data from eleven sub-basins were integrated with contemporary stream gauging data from UH/ASPA efforts. The integrated streamflow dataset included a total of fifteen sub-basins, seven of which had only USGS streamflow records and four of which had only data from UH/ASPA gauges, leaving the remaining four with non-overlapping streamflow hydrographs from both USGS and UH/ASPA records (Fig. 5.7). The runoff component of total streamflow was separated from the baseflow component with the Turning Point Baseflow Separation Method, (Wahl and Wahl, 1995) as described in Barlow et al. (2015). A graphical example of the baseflow separation results are shown in Fig. 5.7.

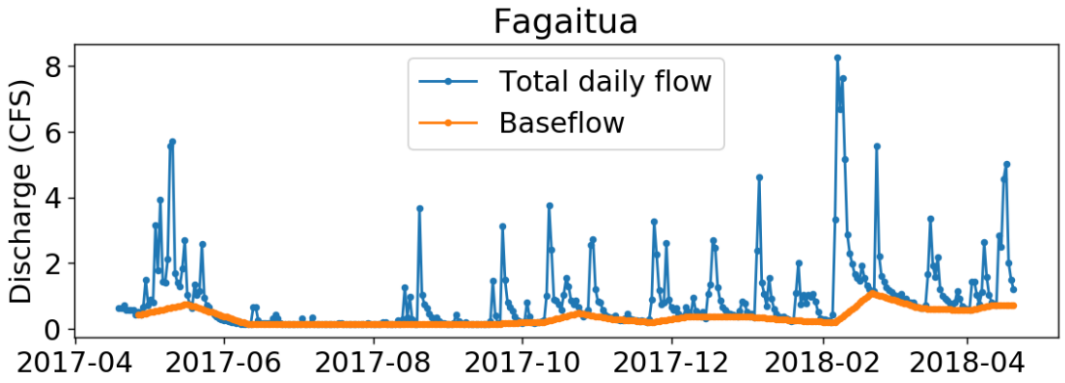

Figure 5.7: Example output of the Turning Point Baseflow Separation Method as performed on the UH/ASPA Fagaitua stream gauge data over a one-year period of record. The orange line indicates stream baseflow in cubic feet per second (CFS), while the blue line indicates total streamflow. Runoff is calculated as the difference between the baseflow and total flow for any given day.

Once the summed quantity of runoff during each month was separated from total stream flow, the runoff amount in each gauged sub-basin was divided by the sub-basin-total rainfall derived from monthly gridded precipitation data (Daly et al., 2006) to yield monthly-resolution R:R ratios. To interpolate R:R ratios to ungauged sub-basins, these measured R:R ratios were assigned to the major watersheds containing each gauged sub-basin, as shown in blue on Fig. 5.8, and watersheds in-between those with measured R:R ratios were assigned

averaged R:R values from the adjacent measured watersheds. If an ungauged watershed was only adjacent to a single measured watershed, then the R:R ratio of the measured watershed was directly assigned to it. This process was extended to each major watershed until a measured or interpolated R:R ratio was assigned in every watershed on the island, except in the Tafuna-Leone plain region where this method was modified to account for unique geologic conditions.

The geologic youth of the Tafuna-Leone basalts and the low slope of the plain's topography both contribute to a significantly higher hydraulic conductivity in this area (Davis, 1963; Bentley, 1975). This causes a reduction in runoff to rainfall ratios and thereby an increase in net-infiltration rates, an effect which has been previously described by Izuka et al. (2007) and Perreault (2010). This causes the plain's few developed stream channels to typically remain dry except during the heaviest rain events, making measurement of streamflow in the Tafuna-Leone region difficult. Thus there are currently no estimates of runoff in this the Tafuna-Leone area. Both Izuka et al. and Perreault assumed that most of the runoff in the plain likely infiltrates before running off, and they estimated this quantity to be approximately 75% of the total runoff generated in this region. For this study, the same assumption was made as no other information to better approximate this value was available. This was accomplished by multiplying the R:R ratio in each watershed adjacent to the Tafuna and Leone Plains, respectively, by a constant factor of 0.25 to obtain estimated R:R ratios in these areas.

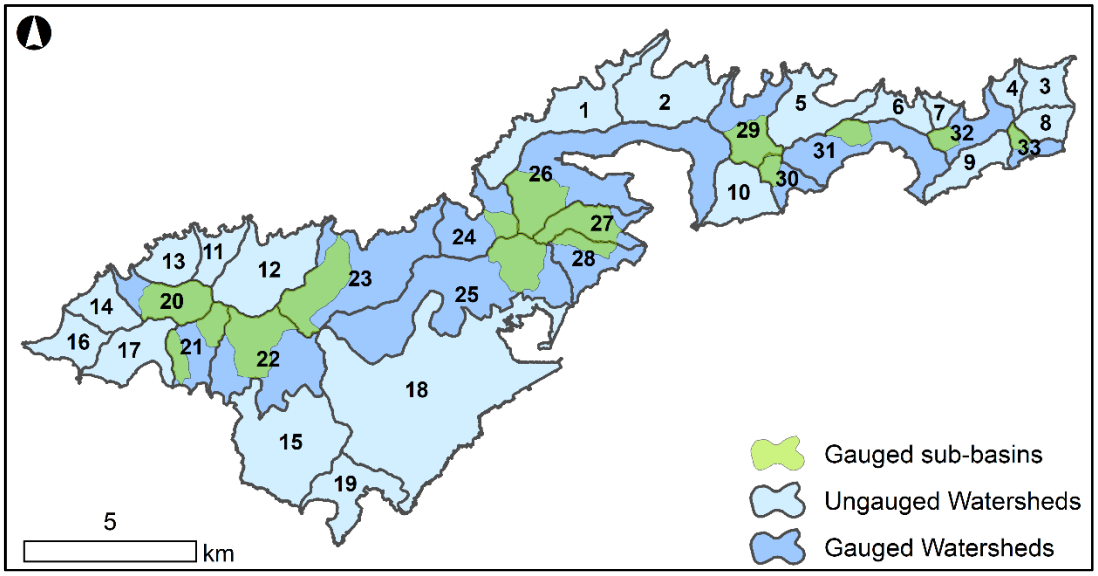

Figure 5.8: Measured sub-basins (green), major watersheds containing at least one continuous record stream gauge (dark blue), and ungauged major watersheds (light blue) lacking stream gauges. Labels indicate zone code number.

To assess the validity of this method, the R:R ratios calculated in this study were compared to ratios independently calculated by Perrault (2010), who determined R:R ratios for the eleven USGS streamflow records using baseflow separation method of (Wahl and Wahl, 1995), and sub-basin-total rainfall derived from Daly et al. (2006). In general, both datasets compared reasonably well, with the average relative percent differences (RPD) between R:R ratios at each station equaling about 10%, and with the correlation coefficient (r^2) of the regression between the two datasets equaling 0.74 (Fig. 5.9). Note that the RPD is calculated as the difference between two values divided by the average of the two values.

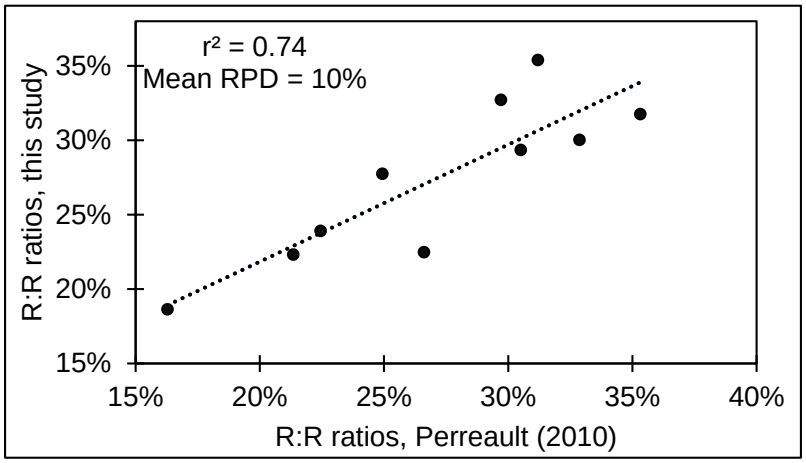

Figure 5.9: Comparison of runoff to rainfall ratios (R:R ratios) calculated in this study to those calculated by Perreault (2010), for the ten watersheds that both studies commonly assessed.

5.2.6 Direct Infiltration

Anthropogenic activities have the potential to significantly affect the spatial distribution of water balance components through water use, infrastructure leakage, and wastewater disposal. Unfortunately for sustainable water management goals, a significant fraction of the water produced by municipal wells is lost to underground water leakage from aging distribution mains and service laterals. This loss is referred to as non-revenue water (NRW). To assess the quantity of leaked NRW, total water production and consumption rates were obtained from ASPA. Over the last 5-years, island wide water production has ranged between 7.3 and 12.8 million gallons per day (Mgal/d) with an average of 10.8 Mgal/d. Customer service records indicate total metered-water use for the same period has averaged approximately 4.7 Mgal/d. Thus as of April 2018, the total island wide NRW was about 6 Mgal/d or about 55% of all water produced from pumping wells on Tutuila.

To model the contribution of NRW to groundwater recharge, the island-wide NRW total of 6 Mgal/d was distributed equally over all model cells that intersected with a water main. Locations of water mains were provided by ASPA in a georeferenced vector format. To

calculate the appropriate depth of NRW in each of the intersecting SWB2 grid cells, the island-wide NRW volume was divided by the number of cells intersecting a water line, and again divided by the area of each grid cell. This calculation yielded a depth of NRW water (in m/day) for each water-line grid cell, and was directly added to the infiltration component of the model (Fig. 5.10). It should also be noted that this method assumes that all water lines leak, and that they leak at an equal rate. Information regarding where subsurface leaks are actually located is lacking, thereby hindering a more accurate assessment of the spatial distribution of water leaks. However, the assumption we adopted here was considered reasonable considering the high proportion of NRW on the island, which indicates a large proportion of the water delivery system is likely to be compromised.

In addition to NWR, direct infiltration from OSDS leachate was also incorporated into the model. This was accomplished by indirectly determining the probable locations of OSDS units through geospatial subtraction of home or business sized buildings (> 120 m^2) located within 10 m of a wastewater main or lateral. Note that the most recent geospatial Tutuila building location dataset (AS-DOC, 2009) was obtained from the American Samoa Department of Commerce (AS-DOC), and the locations of wastewater lines were provided by ASPA. Buildings larger than 120 m^2 and located more than 10 m away from a sewer line were assumed to require an OSDS unit for wastewater disposal. Per-unit effluent discharge rates from Shuler et al., (2017), equaling 1.45 m^3/d per OSDS unit, were applied to calculate the total volume of additional water discharged by OSDS units in each grid cell. Island wide, the number of estimated OSDS units was approximately 5,750, which when multiplied by the above discharge rate, yielded a total OSDS discharge volume of about 2.2 Mgal/d. Effluent volume at each cell was converted to depth of water in the same manner as the additional NRW infiltration (Fig 5.11). Both NRW and OSDS effluent additions were supplied to the SWB2 model in a grid format, and were directly added to the calculated net-infiltration in each model cell.

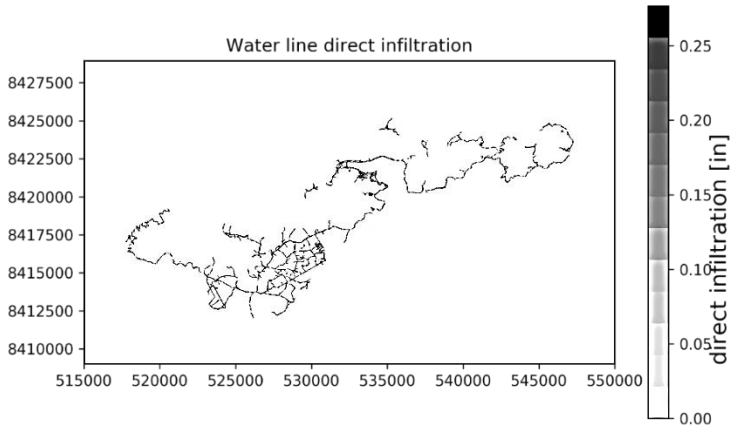

Figure 5.10: Estimated direct net-infiltration rates from leaking water lines, i.e. non-revenue water (NRW).

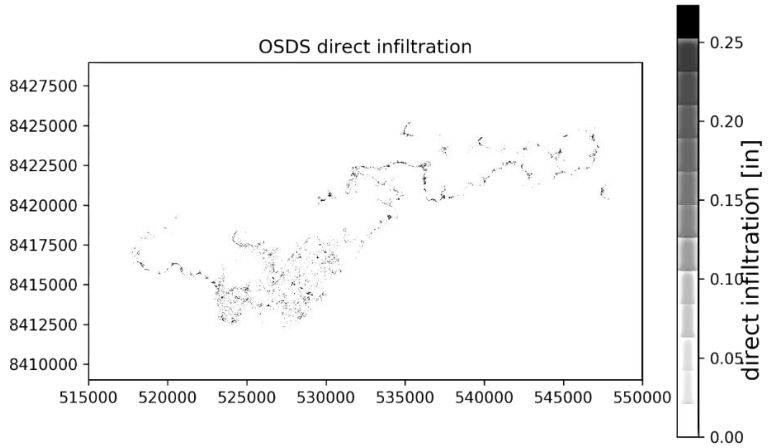

Figure 5.11: Estimated direct net-infiltration rates from OSDS discharge.

5.2.7 Potential Evapotranspiration

The SWB2 model has the ability to develop estimates of potential evapotranspiration (PET) from maximum and minimum air temperature data. However, if existing gridded monthly PET data exist, these data can be directly supplied to the model. Fortuitously, PET maps for Tutuila were previously developed by Izuka et al. (2005). This study used the Penman (1948) method to analyze climate and pan-evaporation measurements from nine measurement stations throughout Tutuila to produce monthly PET maps for Tutuila Island (Fig. 5.12). For this study, these PET maps were first vectorized then converted to a gridded raster format with a spline interpolation method, so that they could be directly supplied to the SWB2 model. To determine actual evapotranspiration rates (AET), the SWB2 model was set to use the FAO–56 Method (Allen et al., 1998), which essentially sets AET values equal to PET values until soil moisture reaches a threshold value near the soil-wilting point, at which point the AET begins to linearly decrease with time to zero.

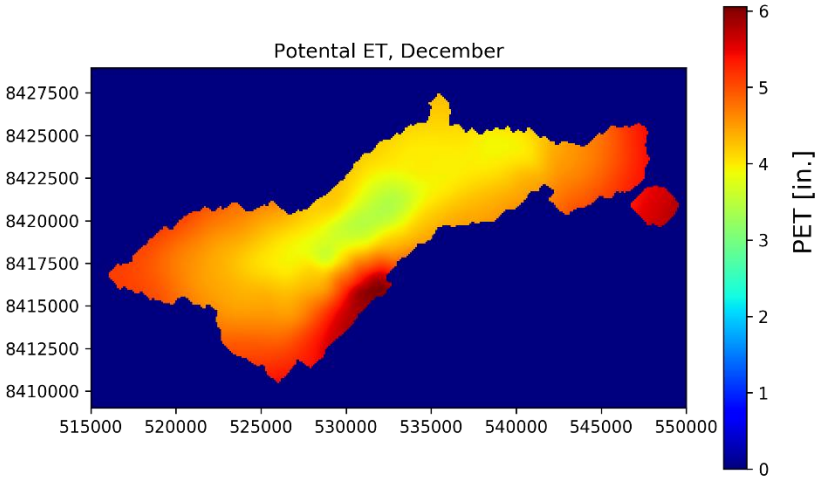

Figure 5.12: Gridded monthly potential evapotranspiration map for the month of December. Data was derived from hardcopy maps taken from Izuka et al. (2005).

5.2.8 Canopy Interception and Losses

As precipitation falls on a forested landscape, most raindrops are intercepted by vegetation before reaching the land surface. While much of this water ultimately falls to the forest floor, a proportion of it evaporates while still on vegetative surfaces. This process, termed canopy evaporation, is defined as the amount of intercepted precipitation that evaporates from leaves, stems, and trunks of a forest. The SWB2 code provides multiple ways to model interception and evaporative losses in forested areas. Because the Gash et al. (1995) conceptual model and computational method was determined to be most applicable to the tropical forests modeled in the Maui case study (Westenbroek et al., 2018) this method was chosen to represent canopy processes on Tutuila as well. The Gash method assigns parameters controlling canopy cover, canopy storage capacity, trunk-storage capacity, and the proportion of precipitation diverted to stem-flow to forested land-use zones. With this method, canopy interception is calculated on a daily-time step where water that remains in canopy or trunk storage after precipitation has stopped is subject to a user specified canopy evaporation rate.

The Gash et al. (1995) method requires canopy evaporation data to calculate evaporative losses from the canopy over the course of modeled rainfall events. On Oahu, estimated-gridded canopy-evaporation data have been successfully developed by applying an empirically derived linear relationship between average annual wind-speeds and annual rainfall rates (Engott et al., 2015). Therefore, to develop estimates of average annual canopy evaporation on Tutuila, the same linear model between rainfall and wind speed at 30 m height that was previously described for the island of Oahu, was applied for Tutuila for input in the SWB2 model (Fig. 5.13).

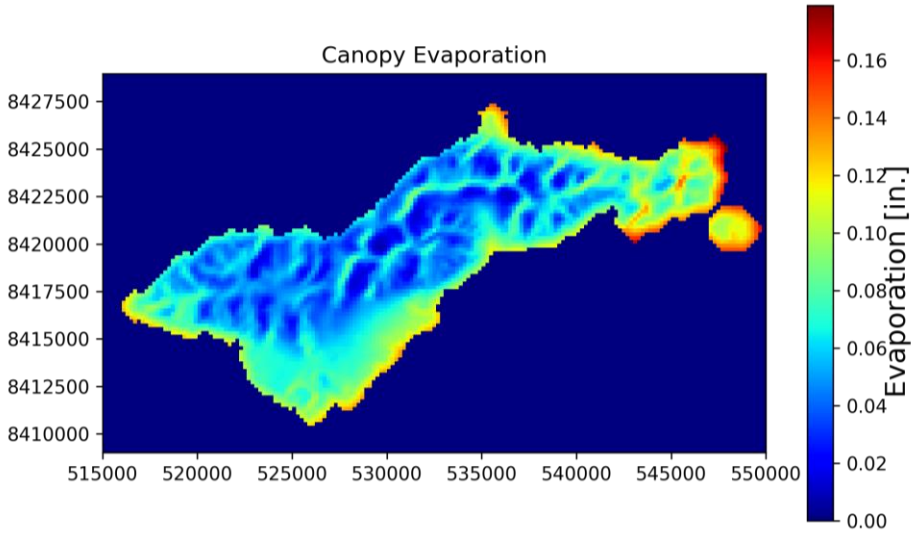

Figure 5.13: Processed map of canopy evaporation derived from average annual wind speed and average annual precipitation gridded datasets.

5.2.9 Mountain Front Recharge

Infiltration on the Tafuna-Leone Plain is enhanced by the process of Mountain Front Recharge (MFR), where surface waters and overland runoff from watersheds above the plain infiltrate into streambeds or soil once reaching a more permeable geologic substrate. This process is analogous to the MFR frequently observed in arid climates (Wilson and Guan, 2004). On the highly-permeable Tafuna-Leone Plain, the majority of direct precipitation has been observed to infiltrate before it has a chance to runoff due to the high permeability of the Holocene-age lavas (Perreault, 2010). There are only a few well developed stream channels on the plain and no perennial streams. In contrast, the older volcanic shields that lie above the plain have much lower permeabilities and contain perennial streams and springs that drain to the sea or terminate at the Tafuna-Leone Plain (Izuka et al., 2007). Actual points of infiltration likely vary depending on stream discharge or rainfall rate, thus a MFR zone located at the base of the mountains has been previously defined (Izuka et al., 2007; Perreault, 2010). While MFR is most significant in the Tafuna-Leone Plain, it has also been observed to a limited extent in Tutuila's alluvial-fill valleys.

The MFR process was simulated in this work by calculating the total volume of runoff produced within an MFR capture area above the Tafuna-Leone Plain, and applying a fraction of this runoff as direct infiltration within the downgradient MFR zone. The MFR infiltration zone boundaries were delineated by Izuka et al. (2007) as the northern portion of the Tafuna-Leone plain that lies within the Pavaiai stony clay loam soil unit, as surveyed by Nakamura (1984). This soil unit overlies the highly conductive Tafuna-Leone lavas and was described as a deep, well-drained soil with moderately high permeability. The area along the floor of Malaeimi Valley was also included in the MFR infiltration zone for this study, based on direct observations of streams infiltrating into the ground in this area. The extent of the MFR capture area included the watershed boundaries between the mountain crest and the northern boundary of the MFR infiltration zone is illustrated in Fig. 5.14. Izuka et al. (2007) and Perreault (2010) previously estimated that 75% of runoff generated in the MFR capture zone likely soaks in to the infiltration zone, and because there exists no new information to update this assumption, the total volume of MFR added as direct infiltration in the MFR infiltration zone (7.6 MGD) was calculated as 75% of the MFR capture-zone runoff from a preliminary run of the SWB2 model.

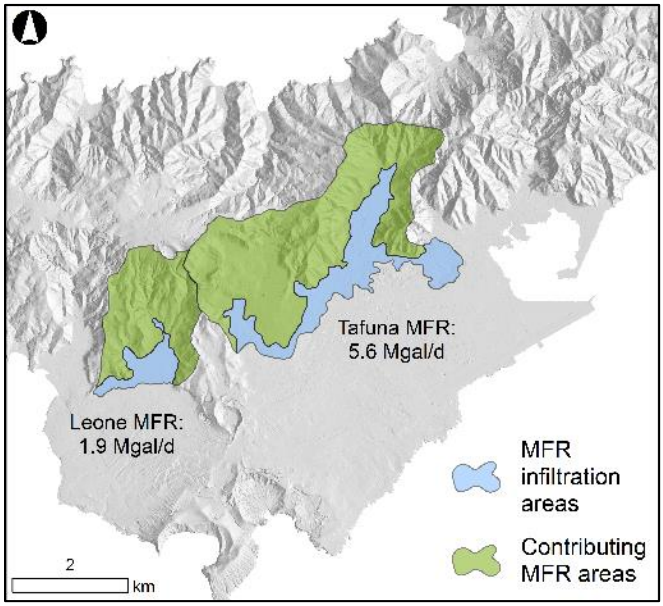

Figure 5.14: Mountain front recharge (MFR) capture and infiltration zone boundaries for the Tafuna and Leone sides of the Plain as applied to the SWB2 model. Total volumes of MFR added to model cells within each MFR infiltration zone are labeled.

5.3 Results and Discussion

The SWB2 model produces spatially and temporally-distributed datasets for each output parameter in a NetCDF file format. Each NetCDF file contains one spatially-distributed gridded dataset for every day for which the model was run. Because the Tutuila model was run for a total of ten years, each Net CDF file contained 3653 two-dimensional grid files, each of which specified a depth of water (in inches) for the given parameter at each grid cell during each of the modeled days. For interpretation, these highly distributed multi-dimensional datasets were summarized by first calculating average annual water depths in each cell to create an average annual gridded dataset for each parameter. The output datasets were then summarized spatially by calculating the total volume of water contained in each component on an island-wide scale, as well as calculating the total volumes of water in each component within each major watershed on the island. Annual gridded-parameter datasets are shown below in Figs. 5.15 to 5.20. At the annual, whole-island resolution, the water budget model can be conceptualized as a simple equation, despite the more complicated internal daily processing steps. This equation takes the form:

$$Water\ inputs = Water\ outputs$$

On the water input side, precipitation inputs equaled 394 Mgal/d (as an annual average), which was summed with an additional 8 Mgal/d of water representing direct infiltration due to OSDS and leaking water line discharge. Together, these represent an initial water input value of 402 Mgal/d. For this work, the MFR amount was calculated as a function of the runoff component from the watersheds above the Tafuna-Leone Plain. Therefore, an initial model run was performed to determine the quantity of MFR, which totaled 7.6 Mgal/d. This volume of water was distributed to the MFR infiltration zones as direct recharge during the second and final model run.

Significant water budget components on the water outputs side included canopy interception, AET, runoff, and net infiltration. Of these, SWB2 calculated a loss of 33 Mgal/d or 8% of total water inputs to canopy interception, and a loss of 61 Mgal/d or 15% of water inputs to evapotranspiration, as determined by soil-moisture processing. Island wide runoff was initially calculated to be 92 Mgal/d or 23% of total water inputs, of which 5.7 Mgal/d was captured and re-introduced to the model as MFR, thereby reducing the amount of water lost to runoff to 86 Mgal/d or 21% of water inputs. This left the remaining 54% of inputs, totaling 221 Mgal/d, as the total island wide net-infiltration estimate. When summed, all output parameters yielded 399 Mgal/d, which accounts for 99.4% of the 402 Mgal/d of water inputs, thereby leaving a modeled error of less than 1% likely due to rounding error or differences in resolution during results post-processing.

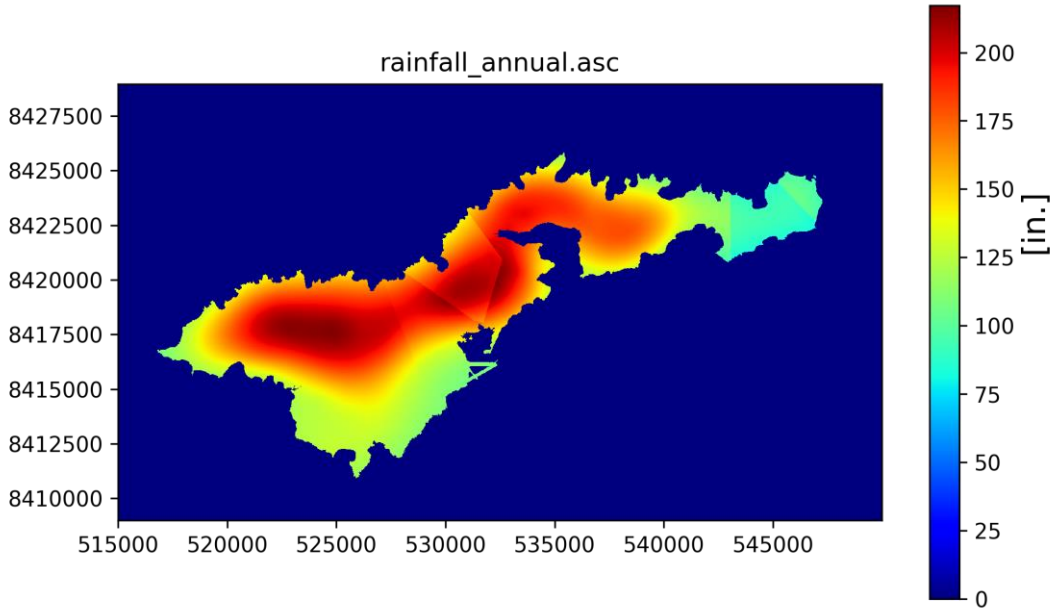

Figure 5.15: Average-annual rainfall after rainfall fragment processing, used as model input.

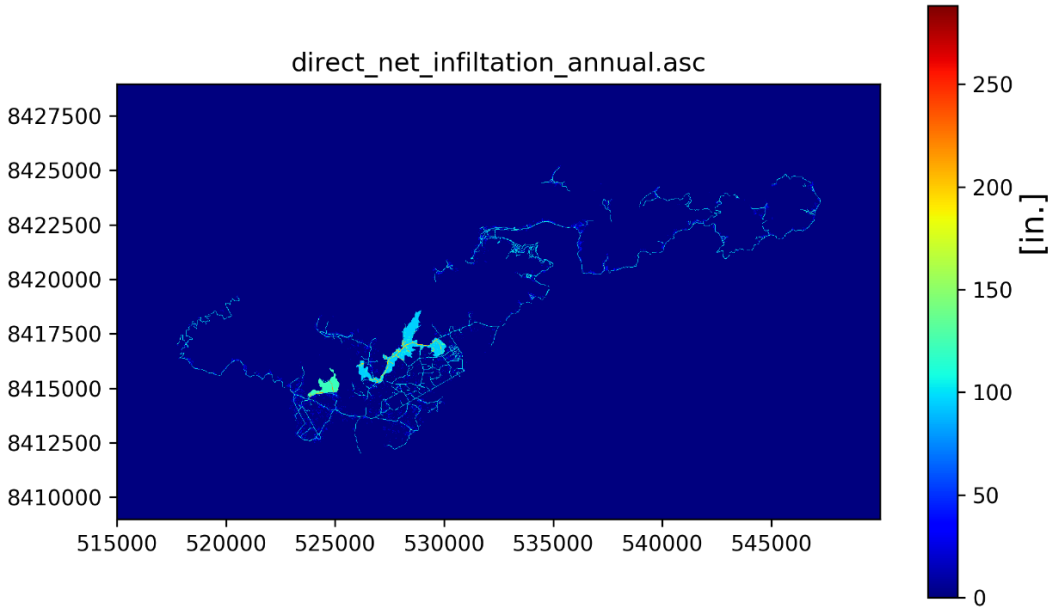

Figure 5.16: Final average-annual direct infiltration additions from OSDS effluent, leaking water lines, and MFR.

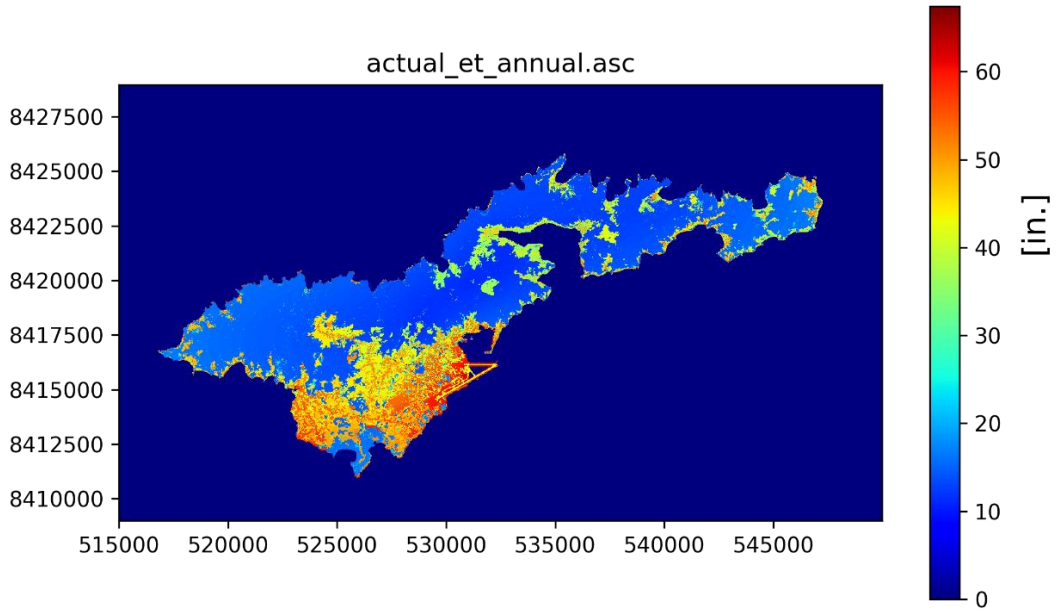

Figure 5.17: Final model output of average-annual actual evapotranspiration (AET).

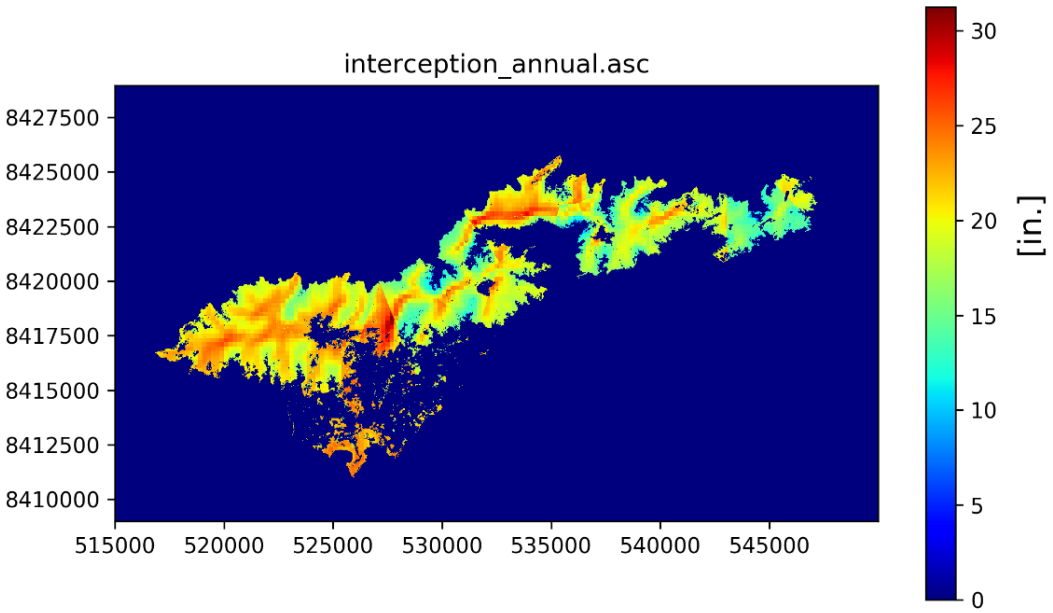

Figure 5.18: Final model output of average-annual canopy interception and subsequent evaporative losses.

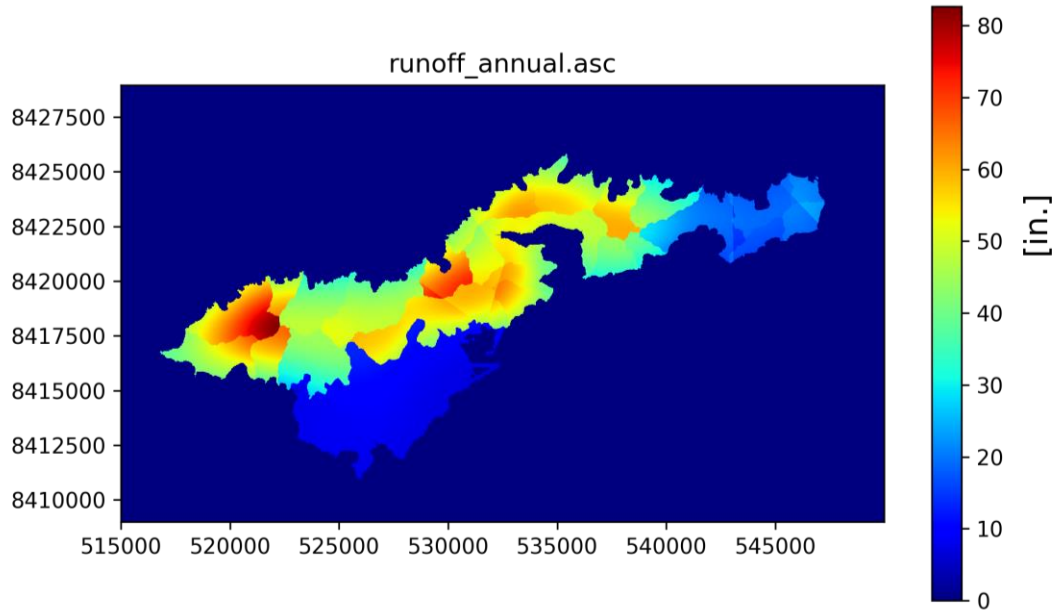

Figure 5.19: Final average-annual runoff totals.

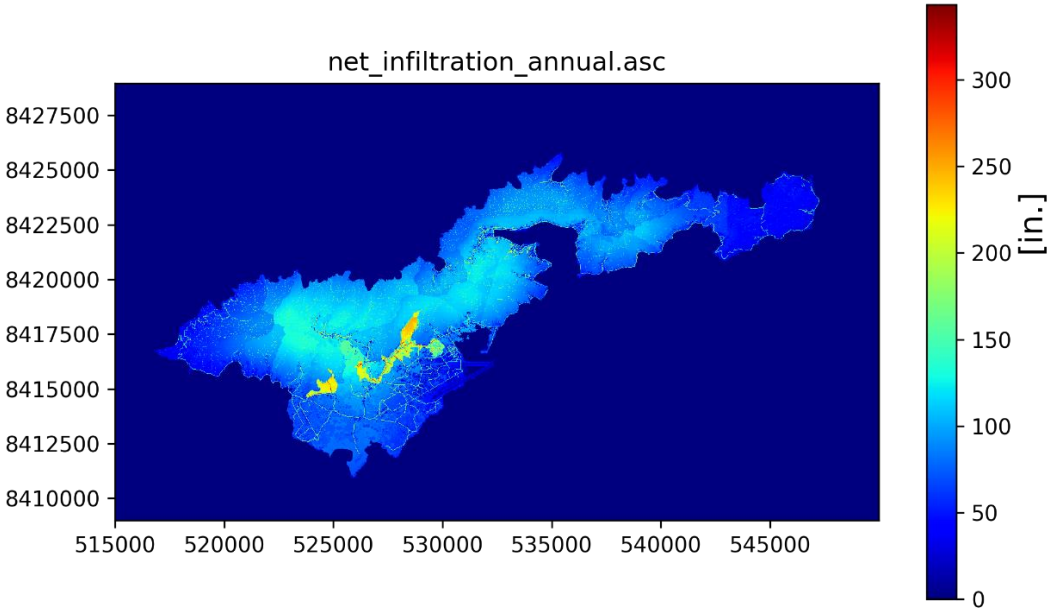

Figure 5.20: Final model calculated net-infiltration, presented at an annual average resolution. Also see Fig, 5.26 for a high resolution detail map of this net infiltration result.

5.3.1 Future Climate Scenarios

The water budget calculations discussed so far utilize climate data collected in the late 20th and early 21st centuries, and therefore represent estimates of hydrologic conditions during this period. However, the climate of the late 21st century, and likely beyond, will undeniably be significantly different than it has been in the short period of time since the start of the industrial revolution. The availability of water resources will be most affected by changes in amount and distribution of rainfall, as well as an increase in temperature, which is a major driver of ET. To estimate the potential effects of future climate change on water budget components, and thus future water resources availability in American Samoa, the Tutuila SWB2 model was run with modified input files derived from dynamically-downscaled climate projections for American Samoa. These projections were developed by Wang and Zhang (2016) using a physically-based global climate model. These authors produced gridded-hourly data for precipitation and temperature at 800 m by 800 m grid resolution and simulated three specific scenarios: (1) present-day climate for the years 1990 to 2009, (2) future climate during the years 2080-2099 reflecting a lower-carbon emissions scenario (RCP4.5), and (3) 2080-2099 climate reflecting on a higher emissions scenario (RCP8.5).

To assess the effects of these possible-future climates on SWB2 calculated net-infiltration rates, the Wang and Zhang (2016) rainfall and temperature projections were transformed into monthly-average grids of rainfall and maximum and minimum average monthly temperatures. The PET calculation method used in the model was also switched so that the effects of higher-future temperatures on ET could be assessed. Note that this method does not include other factors affecting ET such as differences in solar radiation or CO2 concentrations, and this is a limitation with the method. The original model (henceforth referred to as the high-resolution model for reasons explained below) used externally-calculated reference ET values developed with rainfall, temperature, and energy flux measurements taken by Izuka et al. (2005). However, since these values are representative of that study's data collection period and could not be directly recalculated to include modified parameters, a built-in PET estimation method (the Hargreaves-Samani Method) was activated within the SWB2 code to calculate PET during the model run itself. This method utilizes an energy balance approach and is parameterized with user-supplied maximum and minimum air temperature data while applying default values based on vegetation types and latitude-based solar radiation. The effect of changing only the PET method as described above was tested on the high-resolution model, to ensure that the change of ET calculation method would not significantly affect water budget results. When these two methods were tested on an otherwise identical model, the RPD of the run using the Izuka et al. PET values and run using the Hargreaves-Samani calculations was relativity small, at 8.0% for AET and 2.3% for net-infiltration, with all other water budget components having RPD's below 0.1%.

The Wang and Zhang (2016) climate projections included a scenario for the present-day climate (1990 to 2009), but it was found that rainfall totals within this scenario were

significantly lower than present-day rainfall totals measured at physical rain gauge stations and reflected in the precipitation data from Daly et al. (2006), which was used in the original high-resolution model. Additionally, the grid resolution of the of the climate projections dataset (800 m) was much courser than the original high-resolution gridded precipitation input (90 m). Because of these discrepancies, output from the high-resolution model run was not directly comparable to output from the models parameterized with the climate projection datasets. Instead, the percent changes in each water budget component between the downscaled present-day and future (RCP4.5 and RCP 8.5) scenarios were assessed to determine how future climates may, in a relative sense, affect water resources availability (Fig. 5.21 and Table 5.2). If desired, these calculated percent-change values could conceivably be applied to the output from the high-resolution water budget model to produce predictions of volumetric change in water budget components. On an average annual scale, simulation results showed that both of the future climate scenarios predict significant increases in both precipitation and temperature, which translate into overall increases in all water budget components as calculated by the modified SWB2 runs. Most notably, the 11 to 18% increase in precipitation predicted by the RCP8.5 and RCP4.5 scenarios, respectively, drove increases in net-infiltration rates of 17 to 27%, respectively. This would suggest that in the future, the availability of Tutuila's groundwater-resources may significantly improve, though the costs of this will likely also include problems with flooding and groundwater inundation of buried infrastructure. It should also be noted that these results are contingent on the accuracy of these downscaled climate predictions, which do not necessarily represent the only or best predictions available.

Table 5.2: Results for present and future climate scenarios, as well as the results from the original high-resolution model output, given as volumetric totals in upper rows. Lower rows provide the same results but scaled as the percent change between the downscaled-present-day scenario and the future climate scenarios. Note that precipitation totals from the downscaled present-day run are significantly lower than the totals calculated with present-day data from Daly et al (2006), and thus are not directly comparable.

Scenario	Precip. [Mgal/D]	Dir. Infl. [Mgal/D]	AET [Mgal/D]	Intcept. [Mgal/D]	Runoff [Mgal/D]	MFR [Mgal/D]	Net Infiltration [Mgal/D]
High-res. model	393.7	15.7	61.4	33.3	92.3	7.6	220.9
Downscaled: present	228.6	13.3	54.2	31.7	51.9	4.4	105.9
rcp45: 2080 - 2099	269.4	13.9	54.9	34.4	61.2	5.2	134.6
rcp85: 2080 - 2099	253.9	13.6	54.9	33.4	57.8	4.9	123.4

Percent change between downscaled present-day and future climate scenarios, annual averages

Scenario	Precip. [% change]	Dir. Infl. [% change]	AET [% change]	Intcept. [% change]	Runoff [% change]	MFR [% change]	Net Infiltration [% change]
RCP45: 2080 - 2099	17.83%	4.74%	1.15%	8.46%	17.81%	19.23%	27.18%
RCP85: 2080 - 2099	11.06%	2.86%	1.22%	5.22%	11.30%	11.60%	16.57%

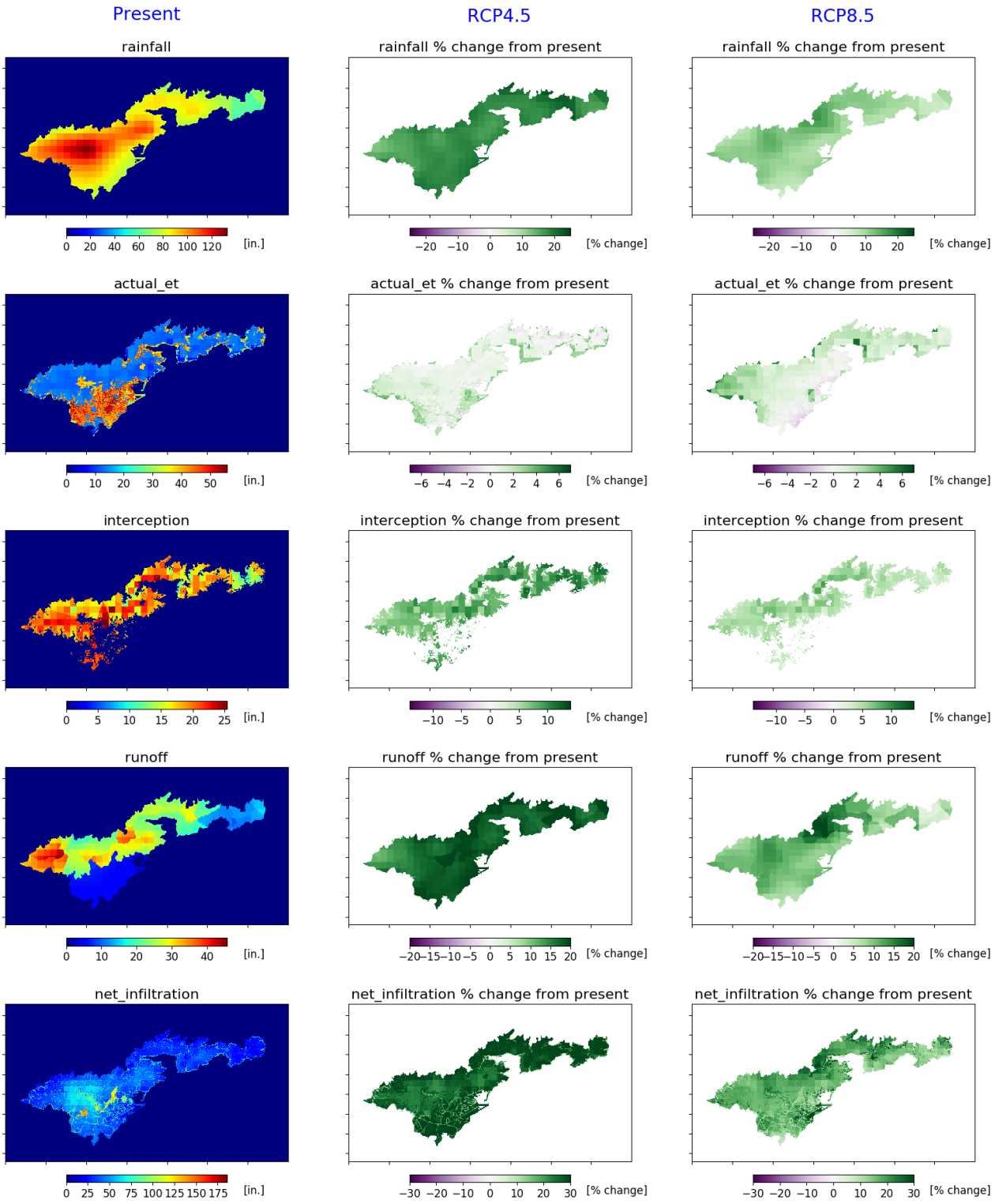

Figure 5.21: Water budget results using downscaled rainfall and temperature predictions (Wang and Zhang, 2016). Present-day predictions are shown as depth of water (left column) whereas future predictions are shown as % change from the present-day scenario for the RCP4.5 (center column) and RCP8.5 (right column) scenarios.

5.3.2 Sensitivity Analysis

Although input datasets and parameter choices used in this model were considered to be those that were most reasonable, uncertainty nonetheless exists in both. Thus, a sensitivity analysis was completed to assess the effect of parameter uncertainty on whole island net-infiltration, as well as to determine which parameters have the most control on model output values. Sensitivity testing only assessed changes in the net-infiltration output, as this parameter is the primary focus of this report.

Parameters chosen for sensitivity analysis included:

- Gridded precipitation
- Tabular runoff to rainfall ratios
- Gridded PET
- Trunk storage coefficient
- Gridded canopy evaporation
- Gridded water line leakage
- Gridded OSDS discharge
- Percent of mountain runoff becoming MFR
- Stem-flow coefficient
- Cell-size
- Flow routing option
- Selection of rainfall fragment sets

For the first nine test parameters listed above, input values were multiplied by test factors of 75%, 90%, 110%, and 125% of the parameter value used in the base case model. When the dataset being tested was formatted as a spatially variable gridded dataset, the entire gridded dataset was multiplied by each test factor and the model was run with each of the modified gridded datasets to test model response through the range of test constants. If the test parameter took the form of single or even multiple coefficients supplied to the model through a lookup table, then multiple lookup tables with the parameter of interest multiplied by each test factor were generated and the model was run with each. Of the eleven tested parameters, three were not formatted in a way that allowed simple multiplication by a constant percentage. The effects of cell-size were tested by running the model with multiple different cell-sizes; the effect of the built-in SWB2 flow routing option was tested by turning the option on and off; and the effect of using different sets of rainfall fragments to develop synthetic daily precipitation sequences was assessed by generating multiple randomly selected fragment sets and comparing output from each one. Detailed descriptions of sensitivity test results are provided below. As mentioned earlier, the sensitivities of results were only limited to net infiltration.

5.3.2.1 Cell-Size

The input file preparation code was set up in a manner that allowed modification of the model cell-size. This not only allowed for faster processing times while building the model, but

also provided the opportunity to determine if cell-size resolution is a factor that affects output parameters. Thus, the model was tested at cell-sizes of 200, 100, 50, and 20 m. Results indicated whole-island model output parameters were only marginally sensitive to cell-size, showing RPD's of less than 7% at 200 m cell-sizes and less than 3% at 50 m cell-sizes (Fig. 5.22), when tested against the base case model at 20 m cell-size. Because a higher-resolution result is often desirable, the final model was run at the lowest practical cell-size, in consideration of model run time and file size (> 35 Gb at 20 m cell-size). Also, because of the small difference between the output at the 20 m and 50 m cell resolutions, all other sensitivity tests were performed at 50 m cell-size to avoid unnecessarily long processing times.

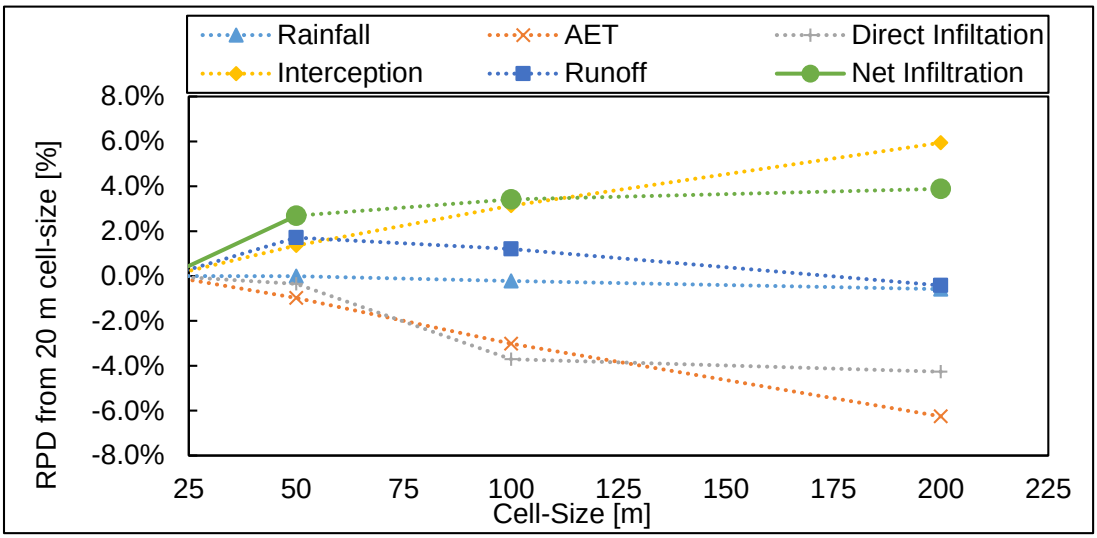

Figure 5.22: Pertinent model output results calculated over runs with different model cell-sizes. Values are shown as relative percent differences (RPD) between values from the model run at 20 m cell-size and the same values at other cell-sizes, up to 200 m.

5.3.2.2 Flow Routing

The SWB2 model contains a flow routing option to more realistically model the transport of surface runoff by considering the effects of steep or hilly terrain on the movement of overland flow. The model uses a D8 flow routing scheme (O'Callaghan and Mark, 1984) that allows surface water generated at a grid cell to flow into the next downslope cell where it is processed along with the runoff component of that cell. Because most water-budget models do not include this option, it was desirable to assess the effects of this method on total net-infiltration. With this method activated, sensitivity testing revealed an increase in island-wide net infiltration by 3.6% (at 50 m cell-size). Therefore, it appears that on an island-wide scale the model is only marginally affected by use of the flow routing method. However, the spatial distribution of infiltration on the sub-basin scale is significantly different as can be seen in Fig.

5.26. This would suggest that this method is most useful in applications where higher resolution results are desired.

5.3.2.3 Rainfall Fragment Set Selection

The Method of Fragments involves randomly selecting different sets of rainfall fragments for each month to generate synthetic daily gridded rainfall datasets from the monthly gridded rainfall data supplied to the model. This method begs the question of how much stochastic variability is introduced through the process of randomly selecting rainfall fragments. To assess this question, the model run time was reduced to one year to maximize the potential variability between different selected sets of rainfall fragments, and the model was run a total of five times, each with a different set of randomly selected fragment sets. Results indicated minimal differences between each model run with RPD between net-infiltration values of < 0.8 %. When all output parameters were assessed, most had RPD values (between each run and the average value of all five runs) of less than 1% with only a few outliers, which were still below 2% (Fig. 5.23). Therefore, this test indicates that selection of different fragment sets will only affect model results by 2% at most, and more likely will affect them by much less considering the final model was run for 10 years, thereby averaging the stochastic variability from each year over the entire time period.

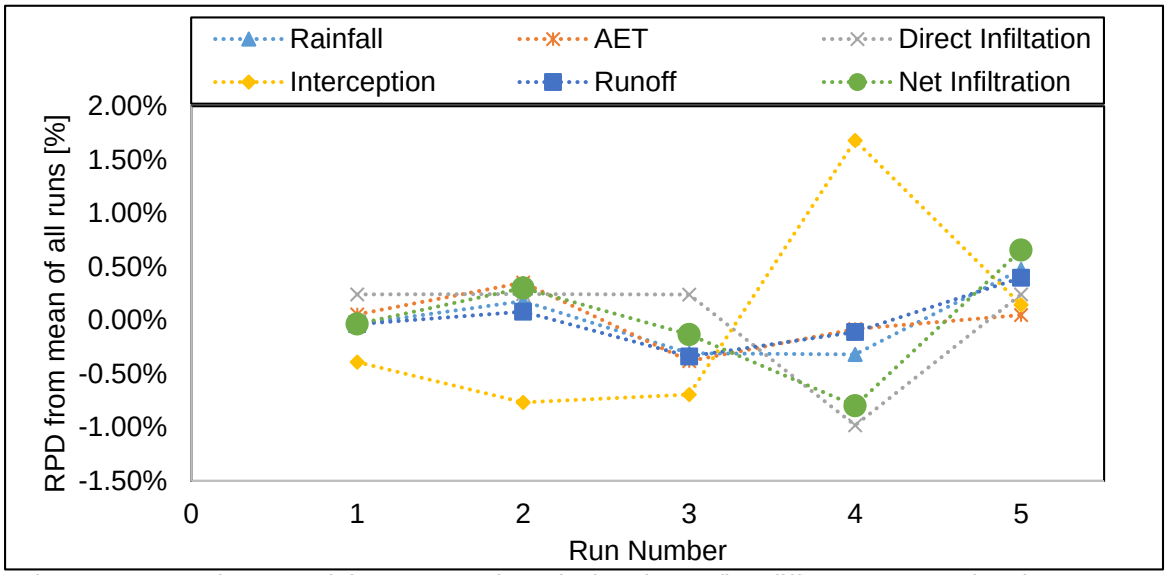

Figure 5.23: Pertinent model output results calculated over five different runs each using a different sequence of randomly selected rainfall fragment sets. Values are shown as the relative percent differences (RPD) between average parameter values across all five runs and the same parameter values for each individual run.

5.3.2.4 Input Parameters Tested with Discrete Constants

Of all input parameters examined with sensitivity testing, the model was only found to be highly sensitive to precipitation inputs, with 'highly-sensitive' meaning that a given percentage change in input values produces a larger percentage change in the net-infiltration output. This result supports the not-unexpected conclusion that rainfall is the strongest control on net infiltration and thus groundwater recharge. The model was less sensitive to all other parameters, with the next most important ones bring runoff and PET. Changes in all other parameters tested with these constants yielded relative changes in output that were less than $1/10^{th}$ of the magnitude of the change in the input parameter. Table 5.3 shows the RPD in net infiltration values between the base case model run and each of the sensitivity test runs for the gridded or look-up table values.

Table 5.3: Sensitivity test results expressed as relative percent differences (RPD) in model calculated net infiltration between the base case model and sensitivity test runs. For each parameter, individual model input parameters were multiplied by test constant values of 75%, 90%, 110% and 125%. Values for RPD are based off of the difference between net infiltration calculated in the base case model run and net infiltration from the run where the given input parameter was multiplied by each test constant.

Input parameter undergoing change	Input values x 75%	Input values x 90%	Input values x 100%	Input values x 110%	Input values x 125%
	Relative percent difference in modeled net infiltration values				
Precipitation [RPD]	-37.81%	-13.65%	-	12.06%	27.68%
R:R ratios [RPD]	8.22%	3.37%	-	-3.48%	-8.92%
PET [RPD]	5.82%	2.31%	-	-2.27%	-5.61%
Trunk storage [RPD]	1.98%	0.79%	-	-0.78%	-1.94%
Canopy evaporation [RPD]	1.42%	0.55%	-	-0.63%	-1.52%
Water line leakage [RPD]	-0.87%	-0.35%	-	0.34%	0.86%
Percent of mountain runoff becoming MFR [RPD]	-0.66%	-0.26	-	0.26%	0.65%
OSDS discharge [RPD]	-0.24%	-0.10%	-	0.10%	0.24%
Stem-flow [RPD]	0.08%	0.03%	-	-0.02%	-0.05%

5.3.3 Comparison to Previous Tutuila Water Budget Studies

Direct calibration or validation of the SWB2 model was not possible due a lack of sufficient net-infiltration measurements to represent hydrologic processes at the regional scale. Nonetheless, comparisons to previously developed water-budget models can help to provide confidence in this model's results. For the island of Tutuila, only two documented whole island water budget studies (Eyre and Walker, 1991; ASPA, 2013), and one partial-island model covering Western Tutuila (Izuka et al., 2007) were found. The methods of computation, and indeed the accuracy of input datasets appear to be variable between each of the studies. Nonetheless, because of the difficulties inherent in calibration and validation of the water-budget method, it is primarily the user acknowledged reasonableness of input and output data that provides insight into the accuracy of results. The Izuka et al. (2007) study was the only water budget model produced by a national agency (the USGS) in a formally published and internally reviewed format. This study was also the only one of the three comparison studies that included the effects of MFR, and also used daily time-step processing to simulate soil moisture processes. The ASPA model was documented in an internal report within the ASPA-water division. The ASPA study was limited in its explanation of methodologies and appeared to be fairly simplistic in its computational rigor, but unlike the Izuka et al. study, covered the entire island in its extent. The Eyre and Walker study methodology was well documented in a report intended to be publicly available as a USGS report, but was never released. The Eyre and Walker study also covered the whole island in its extent and primarily used simple analytical computations to estimate recharge on a basin-wide scale.

The net-infiltration estimates from each of the three comparison studies were produced in different formats (basin totalization, raster, and vector polygon, for the Eyre and Walker (1991), ASPA (2013), and Izuka et al. (2007) studies, respectively), thus the output of each was converted into a standardized format to assess the reasonableness of the magnitude and spatial distribution of recharge to that of this study (the SWB2 model). This was done by summing total net-infiltration within the boundaries of each major watershed to obtain a basin total infiltration rate for each. A summary of watershed-scale comparisons is shown in Fig. 5.24 and basin-total net-infiltration rates are presented graphically in Fig 5.25. In general, correlation coefficients (R^2) between the SWB2 model and the other studies are high, indicating the spatial distribution of recharge is similar in all studies. However, only the Izuka et al. comparison had a linear regression slope close to 1, whereas the regression slopes are around 1.4 in comparisons to the other two models, indicating these models, comparatively, are systematically under-predicting infiltration rates. This may be due to the addition of MFR in the SWB2 and Izuka et al. models, but not in the other two. The RPD in calculated net-infiltration rates between the watersheds from each study provided another way to directly compare models on the watershed scale. This analysis yielded a mean RDP between the SWB2 and the Izuka et al. model of only 17%, while mean RPDs between the SWB2 model and the ASPA and Eyre and Walker models were 67% and 107%, respectively. Overall, the high R^2 low RPD, and the linear-regression slope between the Izuka et al. and SWB2 models suggests that the results of both of these models are fairly reliable.

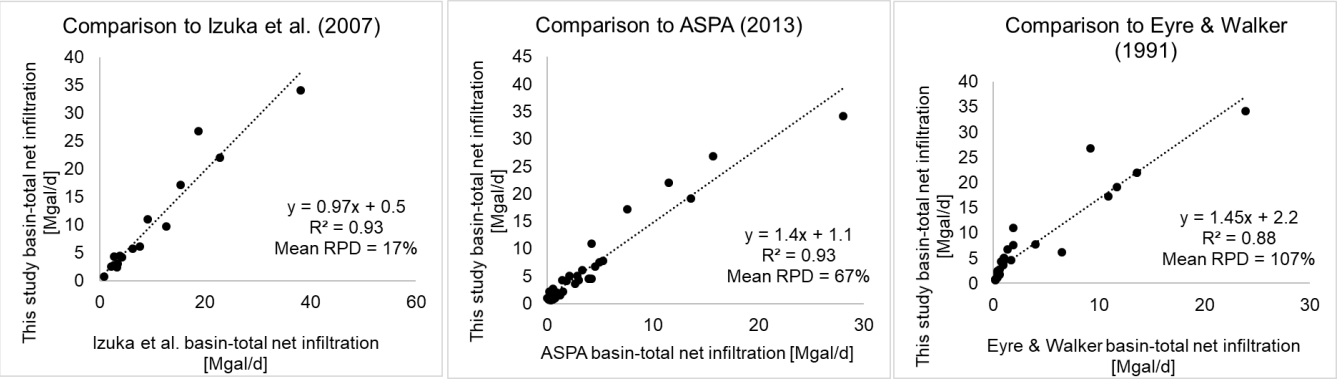

Figure 5.24: Quantitative comparisons of watershed-total net-infiltration amounts between the SWB2 model of this study and the three available Tutuila water-budget model comparison studies of Eyre and Walker (1991), ASPA (2013), and Izuka et al. (2007).

5.4 Summary and Conclusions

The SWB2 water budget model code created by the USGS (Westenbroek et al. 2018) was developed to specifically address unique hydrologic processes occurring in a wide array of settings, with a specific emphasis on high-tropical islands. For this study, the SWB2 code was applied to the island of Tutuila in American Samoa in order to calculate water budget components with a focus on net-infiltration, as this parameter directly relates to water resources availability via groundwater recharge. Water inputs to the model included monthly-gridded precipitation data developed by the PRISM Group (Daly et al., 2006) as well as direct-net infiltration resulting from anthropogenic sources such as leaking water lines and OSDS discharge. Land use, soil type, land slope, PET, wind speed, and surface water flow data were also used to parameterize the model. The SWB2 model used a stochastic approach where random sets of monthly rainfall patterns were used to disaggregate monthly-gridded precipitation data into a sequence of synthetic daily-gridded precipitation inputs, allowing the model to perform soil-moisture processing on a daily time step. The daily-resolution output was subsequently post-processed to reflect annual average totals of water budget components, and also within each major watershed on the island. The calculated water-budget components of interest included precipitation, ET, canopy interception, direct net-infiltration, runoff, and net infiltration. Results indicate 54% of Tutuila's rainfall ends up infiltrating to be available as potential groundwater recharge, 8% is lost to canopy evaporation, another 15% is lost as ET from soils, and 21% is lost as stormflow-runoff to surface water features.

Sensitivity testing revealed that rainfall was the parameter to which the modeled net-infiltration result was the most sensitive. This was followed by the R:R ratios and PET. Variation in other parameters by 25% yielded changes in net infiltration of less-than 2%, suggesting the model was not very sensitive to these parameters. Therefore, high uncertainties in poorly constrained parameters, such as MFR ratios and the spatial distribution of NRW leakage are mitigated by the lack of sensitivity to these parameters in final recharge results. On the other hand, the model is more sensitive to R:R ratios, and the measurement uncertainty is likely to be high on this parameter,due to uncertainty in the empirical relationships used to calculate streamflow and the subjectivity inherent in baseflow-separation analysis. Conversely, even though the model is most sensitive to precipitation, the uncertainty on this parameter is probably fairly low, as it was interpolated from numerous measurement stations and averaged over a 30-year period. Therefore, the model's weakest link is probably the R:R ratios. This indicates that future efforts targeted at developing better constraints of streamflow, especially in MFR affected areas would be very useful for improving estimates of groundwater recharge.

The effects of future climate change on water resources availability was also tested with the parameterized water budget model. This was accomplished by integrating dynamically downscaled climate predictions for 2080 to 2099 derived from a global climate model (Wang and Zhang, 2016) into the SWB2 model input files. Specifically, modified rainfall and temperature datasets were supplied to the model, and an increase in net-infiltration of 17 to 27% was predicted depending on the emissions scenario used. Sensitivity testing was performed with all model parameters and the effect of precipitation was found to have the most impact on net-infiltration amounts. Model results were validated by comparison to three other previously documented water budget models and the SWB2 model produced results that were reasonably consistent with the most reliable of the previous models, showing an average RPD of just 17% for overlapping watersheds.

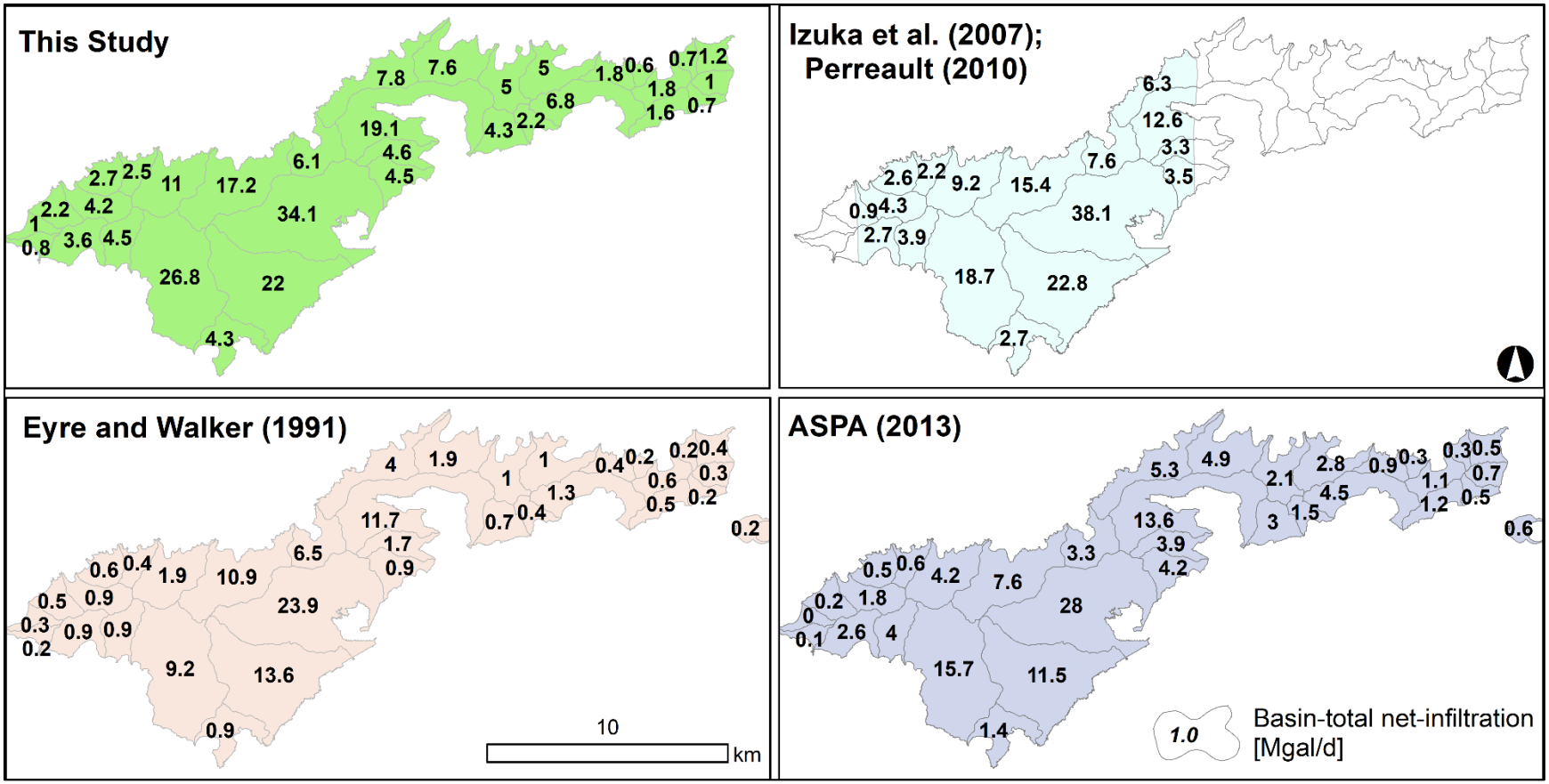

Figure 5.25: Comparison of basin-total net-infiltration amounts, in Mgal/d, between this study and three other documented Tutuila water-budget models. Only the model from Izuka et al. (2007) study was formally published, with the other two being contained in unpublished reports. Also the Izuka et al. model is the only other one that includes the effects of MFR on the Tafuna-Leone Plain.

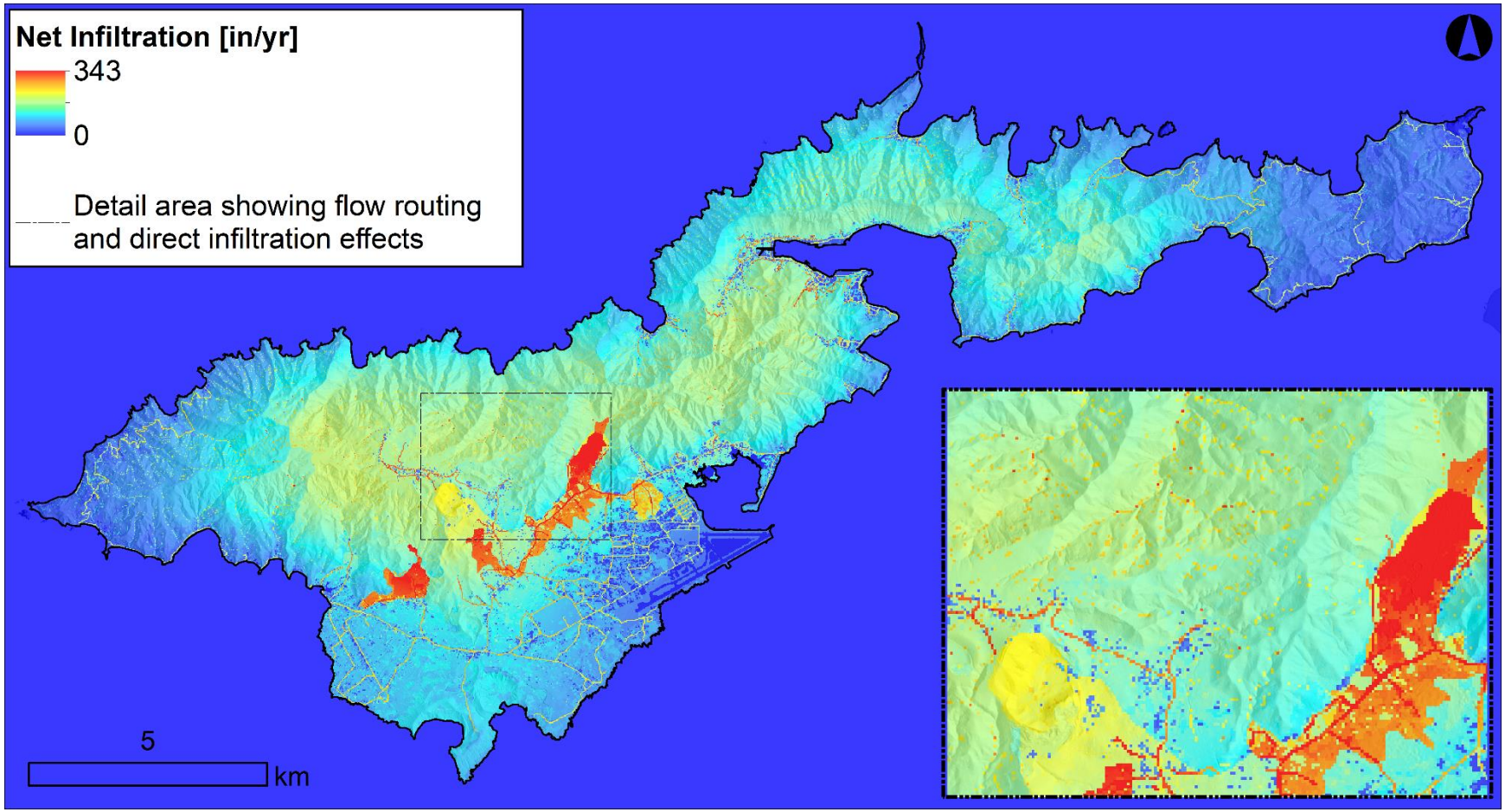

Figure 5.26: Detail map of model calculated average-annual net infiltration at 20 m cell-size resolution. Inset map shows detail of (1) flow routing effects, seen as higher recharge squares at the bottom of drainage channels, (2) direct infiltration from leaking water lines, seen as linear zones of higher infiltration, and (3) MFR zones seen as larger patches of high-infiltration.

5.4.1 SWB Technology Transfer

The implementation of this model is not intended to be a static-finished product. As different climate projections are developed or updated parameterization datasets are released the model can and should be revised to reflect newer or more accurate data sources. Therefore, the model code and the directory tree with all of the raw-input datasets are hosted at https://github.com/UH-WRRC-SWB-model. This repository contains all the necessary files to completely regenerate the model on any other computer with a Python interpreter and the required modules. To run the model, the user simply needs to download or 'clone' the Github repository (UH-WRRC-SWB-model) and run the code following the instructions in the online-readme file and using a python interpreter such as jupyter notebook. It should be noted that the model was constructed using a number of required python modules, which are listed in the first code block of the model script. All of these modules are open-source except for one, whereas the model uses functionality included with ESRI's ArcPy module, thus the user must have an active ArcGIS or ArcPRO license to run the model and access these functions.

List of input datasets included in repository

- SWB control file: "'Tutuila200_controlFile.ctl"
- Shapefile of model boundary: "grid_bound.shp"
- Shapefile of land use zones: "Land_use_wRO_codes2.shp"
- Shapefile of soil zones: "Tut_Soil_clip2.shp"
- Shapefile of rainfall station Thissen polygons: 'Thissen_poly_rain_clip_modified2.shp"
- Shapefile of watersheds: "All_major_WS_modified3.shp"
- Shapefile of municipal water lines: "Transmission_water_mains.shp"
- Shapefile of OSDS units: "OSDS_units_pts.shp"
- Raster format DEM: "10M_DEM.tif"
- Annual rainfall grid: "An_pcip_in.tif"
- 30 m winds speed map: "wndsp_30m.tif"
- Set of 12 monthly gridded rainfall maps: "PRISM_ppt_tutuila_30yr_normal_80mM1_{ month }_asc.asc"
- Monthly gridded Max temperatures: "PRISM_tmax_tutuila_30yr_normal_80mM1_{ month }_asc.asc"
- Monthly gridded Max temperatures: "PRISM_tmin_tutuila_30yr_normal_80mM1_{ month }_asc.asc"
- Monthly gridded evapotranspiration maps: "'{month}_ET.shp'
- Modified land-use lookup table: "Landuse_lookup_maui_mod5.txt"
- Tabular file of runoff to rainfall ratios: "RO_Rf_ratios_real_monthly3_2000_2010.txt"
- Externally generated rainfall fragment set file: "Rainfall_fragments_2001.prn"
- Sequence file for rainfall fragment order: "Sequence_file_2002.prn"
- Shapefile of mountain font recharge contributing areas: "Contributing_MRF_Areas_leone.shp, Contributing_MRF_Areas_tafuna.shp"
- Shapefile of mountain font recharge receiving areas: "MFR_infiltration_area_leone.shp", MFR_infiltration_area_Tafuna.shp"

Example list of output datasets included in repository

- "actual_et_annual.asc"
- "direct_net_infiltation_annual.asc"
- "direct_soil_moisture_annual.asc"
- "interception_annual.asc"
- "net_infiltration_annual.asc"
- "rainfall_annual.asc"
- "runoff_annual.asc"

References: Chapter 5

Allen, R.G., Pereira, L.S., Raes, Dirk, and Smith, Martin. (1998). Crop evapotranspiration—Guidelines for computing crop water requirements: Rome, Food and Agriculture Organization of the United Nations, FAO Irrigation and Drainage Paper No. 56, 174 p.

Arnold, J.G., Srinivasan, R., Muttiah, R.S., Williams, J.R., (1998). Large area hydrologic modeling and assessment – Part 1: model development J. Am. Water Resour. Assoc., 34 (1) (1998), pp. 73-89, 10.1111/j.1752-1688.1998.tb05961.x.

AS-DOC - American Samoa Department of Commerce. (2009). Buildings layer for Tutuila Island. [Data file]. http://doc.as.gov/

ASPA - American Samoa Power Authority. (2013). Documentation of Wellhead Analysis, Tutuila Hydrogeological Analysis for the U.S. EPA Clean Water Act—State Revolving Fund ASPA Consolidated Grant for the benefit of the Territory of American Samoa. Report prepared for American Samoa Power Authority, Pago Pago, American Samoa. Author Walters, M.O.

Barlow, P. M., Cunningham, W. L., Zhai, T., & Gray, M. (2015). US Geological Survey groundwater toolbox, a graphical and mapping interface for analysis of hydrologic data (version 1.0): user guide for estimation of base flow, runoff, and groundwater recharge from streamflow data. US Department of the Interior, US Geological Survey.

Bentley, C.B. (1975). Ground-water resources of American Samoa with emphasis on the Tafuna-Leone Plain, Tutuila Island. US Geological Survey Report No. 75-29.

Daly, C., J. Smith, M. Doggett, M. Halbleib, and W. Gibson. (2006). High-resolution climate maps for the Pacific basin islands, 1971–2000. Final Report. National Park Service, Pacific West Regional Office.

Davis, D.A. (1963). Ground-water reconnaissance of American Samoa. U.S. Geological Survey Water-Supply Paper 1608-C.

Engott, J. A., Johnson, A. G., Bassiouni, M., & Izuka, S. K. (2015). Spatially distributed groundwater recharge for 2010 land cover estimated using a water-budget model for the island of O'ahu, Hawaii (No. 2015-5010). US Geological Survey.

Eyre, P., and G. Walker. (1991). Geology and ground-water resources of Tutuila American Samoa. Unpublished report in American Samoa Power Authority files.

Gash, J.H.C., Lloyd, C.R., and Lachaud, G., (1995). Estimating sparse forest rainfall interception with an analytical model: Journal of Hydrology, v. 170, no. 1, p. 79–86.

Izuka, S. K., Giambelluca, T. W., & Nullet, M. A. (2005). Potential Evapotranspiration on Tutuila.

American Samoa. U.S. Geological Survey Scientific Investigations Report 2005-5200. U.S. Geological Survey

Izuka, S.K., J.A. Perreault, and T.K. Presley. (2007). Areas contributing recharge to wells in the Tafuna-Leone Plain, Tutuila, American Samoa. Honolulu, HI: Geological Survey (US). Report no. 2007-5167. https://pubs.er.usgs.gov/publication/sir20075167.

Izuka, S.K., Oki, D.S., and Engott, J.A., (2010). Simple method for estimating groundwater recharge on tropical islands: Journal of Hydrology, v. 387, no. 1, p. 81–89.

Izuka, S. K., Engott, J. A., Bassiouni, M., Johnson, A. G., Miller, L. D., Rotzoll, K., & Mair, A. (2016). Volcanic aquifers of Hawai ʻi—Hydrogeology, water budgets, and conceptual models (No. 2015-5164). US Geological Survey.

Johnson, A.G., (2012). A water-budget model and estimates of groundwater recharge for Guam: U.S. Geological Survey Scientific Investigations Report 2012-5028, 53 p

Kennedy, Jenks, and Chilton Consulting Engineers. (1987). Groundwater contamination study Tafuna-Leone Plain Tutuila Island. Final report for the Environmental Quality Commission, Office of the Governor, Tutuila, American Samoa. 168 p.

Mair, A., Hagedorn, B., Tillery, S., El-Kadi, A. I., Westenbroek, S., Ha, K., & Koh, G. W. (2013). Temporal and spatial variability of groundwater recharge on Jeju Island, Korea. Journal of hydrology, 501, 213-226.

Meyer, R.A., Seamon, J.O., Fa'aumu, S., and Lalogafuafua, L. (2016). Classification and Mapping of Wildlife Habitats in American Samoa: An object-based approach using high resolution orthoimagery and LIDAR remote sensing data. Report prepared for American Samoa Department of Marine and Wildlife Resources.

Nakamura, S., 1984. Soil survey of American Samoa. U.S. Department of Agriculture Soil Conservation Service, Pago Pago. 95 p.

National Weather Service (NWS). (2000). Precipitation records from 1971–2000. Data Set.

O'Callaghan, J.F., and Mark, D.M., (1984). The extraction of drainage networks from digital elevation data: Computer vision, graphics, and image processing, v. 28, no. 3, p. 323–344.

Oki, D.S., (2002). Reassessment of ground-water recharge and simulated ground-water availability for the Hawi area of north Kohala, Hawaii: US Department of the Interior, US Geological Survey, 62p.

Penman, H.L., (1948). Natural evaporation from open water, bare soil, and grass: Proceedings of the Royal Society of London, A193, p. 120-146.

Perreault, J.A. (2010). Development of a water budget in a tropical setting accounting for mountain front recharge. Masters Thesis, University of Hawaii at Manoa. Honolulu, HI.

Shade, P. J., & Nichols, W. D. (1996). Water budget and the effects of land-use changes on ground-water recharge, Oahu, Hawaii (Vol. 1412). US Geological Survey.

Shuler, C. K., El-Kadi, A. I., Dulai, H., Glenn, C. R., & Fackrell, J. (2017). Source partitioning of anthropogenic groundwater nitrogen in a mixed-use landscape, Tutuila, American Samoa. Hydrogeology Journal, 25(8), 2419-2434.

Thornthwaite, C.W., and J.R. Mather. (1955). The water balance. Publications in Climatology (Laboratory of Climatology) 8(1): 1–86.

Stearns, H.T. (1944) Geology of the Samoan islands. Geological Society of America Bulletin 55(11): 1279–1332.

Wang, Y. and Zhang, C. (2016). Project Final Report - 21st Century High-Resolution Climate Projections for Guam and American Samoa. Retrieved from: https://www.sciencebase.gov/catalog/item/583331f6e4b046f05f211ae6

Wahl, K. L., and Wahl, T. L., (1995). Determining the Flow of Comal Springs at New Braunfels, Texas, Texas Water '95, American Society of Civil Engineers, August 16-17, 1995, San Antonio, Texas, pp. 77-86.

Westenbroek, S. M., Engott, J. A., Kelson, V. A., & Hunt, R. J. (2018). SWB Version 2.0—A Soil-Water-Balance Code for Estimating Net Infiltration and Other Water-Budget Components (No. 6-A59). US Geological Survey.

Wilson, J.L., and H. Guan. (2004). Mountain-block hydrology and mountain-front recharge. In Groundwater Recharge in a Desert Environment: The Southwestern United States, ed. J.F. Hogan, F.M. Phillips, and B.R. Scanlon, 113–137. American Geophysical Union, Washington, D.C.

Wong, M.F. (1996). Analysis of streamflow characteristics for streams on the island of Tutuila, American Samoa. US Geological Survey Water Resources Investigations Report No. 95-4185, Honolulu, HI.